CHAPTER 4

OPTIMIZATION OF GEOPOLYMER MIX

4.1 General

This chapter discusses the efficacy of GGBS and dolomite-based geopolymer with NH and NS as an alkali activator in the geopolymerization process to stabilize kaolin clay. The effect of precursor content (5%, 10%, and 20%), S:D ratio (20:0 to 16:4), NH:NS ratio (0:100 to 100:0), water content of kaolin clay (0.8LL to 1.2LL), L/P ratio (0.5 to 1.5) and curing time (7 days to 28 days) on the mechanical properties of the stabilized kaolin clay was evaluated using UCS tests, pH tests and CU triaxial tests. The results were compared with OPC stabilized kaolin clay. The microstructural analysis was performed using scanning electron microscope (SEM) and Fourier transform infrared spectroscopy (FTIR) test. On the basis of these influencing parameters, the optimum mix proportions was determined with respect to strength improvement.

This chapter also includes the investigation of the cyclic behavior and the evolution of G and λ of the geopolymer-stabilized kaolin clay under long-term cyclic loading. The influence of geopolymer content (S:D ratio), curing time, CSR, CP, frequency, and possible mechanism are also discussed. Finally, an empirical model for dynamic shear modulus under long-term cyclic loading was proposed to validate the experimental test results. Furthermore, a TCLP test was performed on GGBS, dolomite, and optimum mix specimens to determine the leaching behavior of heavy metals.

4.2 Test Conditions and Variables

This study adopted various combinations of the precursor materials and alkali activators under curing conditions to analyze the effect of different parameters in the geopolymerization process. To analyze the effect of precursor content on the stabilization of kaolin clay for the DSM technique, 5%, 10%, and 20% precursor content (by dry mass of clay) were considered in this study. To investigate the effect of adding dolomite with GGBS for different ratios of alkali activators at different curing times, NaOH: Na_2SiO_3 (NH:NS) mass ratio (100:0, 75:25, 50:50, 25:75, and 0:100); GGBS: dolomite (S:D) ratio (20:0, 18:2, 16:4, and 14:6) considering precursor content of 20%; and curing time (7, 14, and 28 days) were considered. The water content of kaolin clay was set at its liquid limit to simulate the natural water content in the field. Specimens stabilized with 5%, 10%, and 20% OPC at the liquid limit (LL) were also prepared as control specimens for comparison.

Series 4 and 5 investigate the effect of S and D content as a precursor, L/P ratio, water content of kaolin clay, and curing period on the UCS of the geopolymer stabilized kaolin clay. Series 6 depicts the effect of water content of kaolin clay on UCS of the traditional binder (OPC) improved kaolin clay. In series 7, consolidated undrained static and cyclic triaxial tests were performed on selected mix proportions as per the UCS test results. The testing program was conducted in series, as shown in Table 4.1.

Table 4.1 Mix proportion and testing program of specimens.

Parameters		**Series 1**	**Series 2**	**Series 3**	**Series 4**	**Series 5**	**Series 6**	**Series 7**
NaOH	(molars)	8	8	-	8	8	-	8
NaOH: Na_2SiO_3	(L)	25:75	100:0, 75:25, 50:50, 25:75, 0:100	-	25:75	25:75	-	25:75
L/P or water: cement ratio	(L/P) or (w/c)	1.0	1.0	1.0	1.0	0.5, 0.75, 1.0, 1.25, 1.5	1.0	1.0
Precursor / Kaolin clay	(%)	5, 10, 20	20	-	20	20		20
S:D (P)	(%)	20:0	20:0, 18:2, 16:4, 14:6	-	20:0, 18:2, 16:4, 14:6	16:4		20:0, 18:2, 16:4, 14:6
Cement	(%)	-	-	5, 10, 20	-	-	20	-
Water content of LL	(%)	1.0	1.0	1.0	1.2, 1.0, 0.8	1.0	1.2, 1.0, 0.8	1.0
Curing temperature	(°C)	27	27	27	27	27	27	27
Curing time	(days)	7,14,28	7, 14, 28	28	7,14,28	7, 14, 28	28	28
Tests performed		UCS	UCS, pH	UCS	UCS	UCS	UCS	Static and Cyclic triaxial test

4.3 Results and Discussion

4.3.1 Unconfined compressive strength of geopolymer treated soft soil

4.3.1.1 Effect of precursor content

Fig. 4.1 shows the results of unconfined compressive strength of the GGBS-based geopolymer specimens with 5%, 10%, and 20% GGBS content with NH:NS ratio of 25:75, and the results were compared with the 5%, 10%, and 20% OPC stabilized specimens after 7, 14, and 28 days of curing period. Results show that the UCS of geopolymer stabilized specimens increases with an increase in GGBS content for all the curing time. As the treated kaolin clay was very soft with undrained shear strength (c_u) of 2-3 kPa (at the liquid limit), there was a tremendous increase in strength on geopolymerization. This significant improvement in the strength can be attributed to the presence of Ca^{2+} and Al^{3+} in the GGBS, resulting in the formation of the calcium aluminosilicate hydrate (C-A-S-H) gel (An et al. 2022; Hakem et al. 2020; Liu et al. 2023; Min et al. 2023; Su et al. 2023; Zhou et al. 2021). The compressive strength of cement-treated kaolin clay also increased with increased cement content. This improvement in strength was due to the formation and filling of pores in the clay with hydrated calcium silicate hydrate (C-S-H) gel (Cristelo et al. 2013). At all the curing periods, the UCS of GGBS-based geopolymer stabilized clay with 20% GGBS content was 36.4% higher than the 10% OPC (control 2) and lower than the 20% OPC (control 3) treated kaolin clay. By comparing the results, it can be concluded that the increase in precursor content increases the compressive strength of clay along with the curing period.

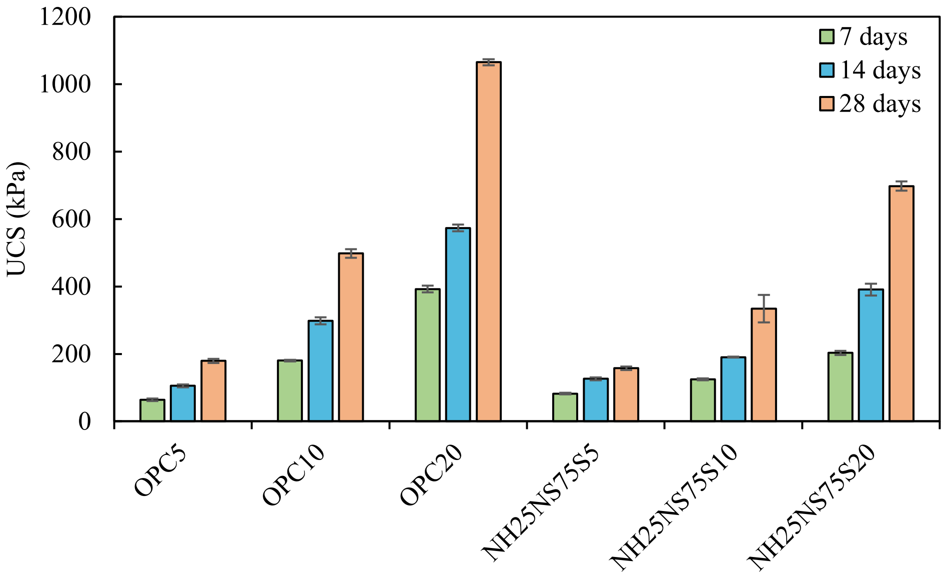

Fig. 4.1 UCS of the geopolymer stabilized specimen with NH:NS ratio of 25:75 and GGBS content of 5%, 10%, and 20% compared with 5%, 10%, and 20% OPC stabilized specimen after 7, 14, and 28 days of curing period.

4.3.1.2 Effect of S:D ratio

To investigate the effect of adding dolomite to GGBS, specimens with different contents of GGBS and dolomite were prepared with different ratios of NH and NS as alkali activators and tested after 7, 14, and 28 days. Fig. 4.2 illustrates the effect of replacing the GGBS with dolomite for different ratios of NH and NS for different curing periods. For all the ratios of NH and NS, an increasing trend of UCS was observed with the increase in dolomite content up to the optimum content. Dolomite makes the geopolymer more conducive to leaching amorphous silica and alumina from clay and GGBS, producing Al^{3+} and Si^{4+} for the geopolymerization reaction due to its high alkalinity (Cohen et al. 2019). The addition of dolomite is highly effective in increasing the compressive strength of kaolin clay, and the maximum strength was observed in NH25NS75S16D4 for all the curing periods. Ca^{2+} is reported to speed up the geopolymerization process by adding more nucleation sites for precipitation, which reduces the setting time (Chen et al. 2023; Cristelo et al. 2011). Replacing the GGBS content with dolomite until reaching the maximum value of 4% increases the UCS value, and a further increase in dolomite reduces the UCS value. A dolomite content of 4% with an NH:NS ratio of 25:75 correlates to the most significant increase in 28 days UCS by 116.8% compared with only GGBS-based geopolymers. As GGBS is the primary source of geopolymerization, the higher the dolomite content, the lower the GGBS content, keeping the precursor content constant. Excessive dolomite content retards the strength development process as more crystals of $Ca(OH)_2$ are formed, which increases the viscosity of the geopolymer solution, which in turn prevents the leaching of silica and alumina ions (Al-kroom et al. 2023; Hanjitsuwan et al. 2020; Ye et al. 2019, 2020).

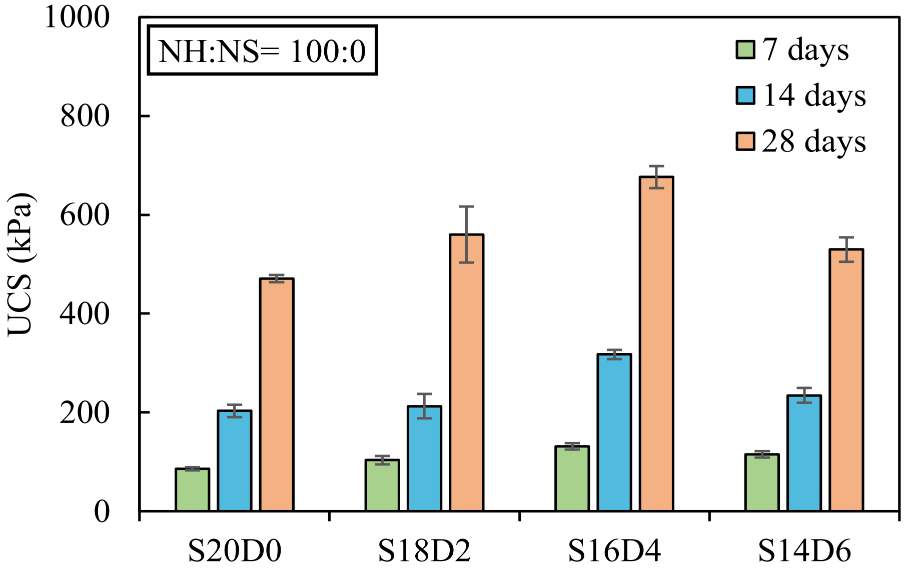

(a)

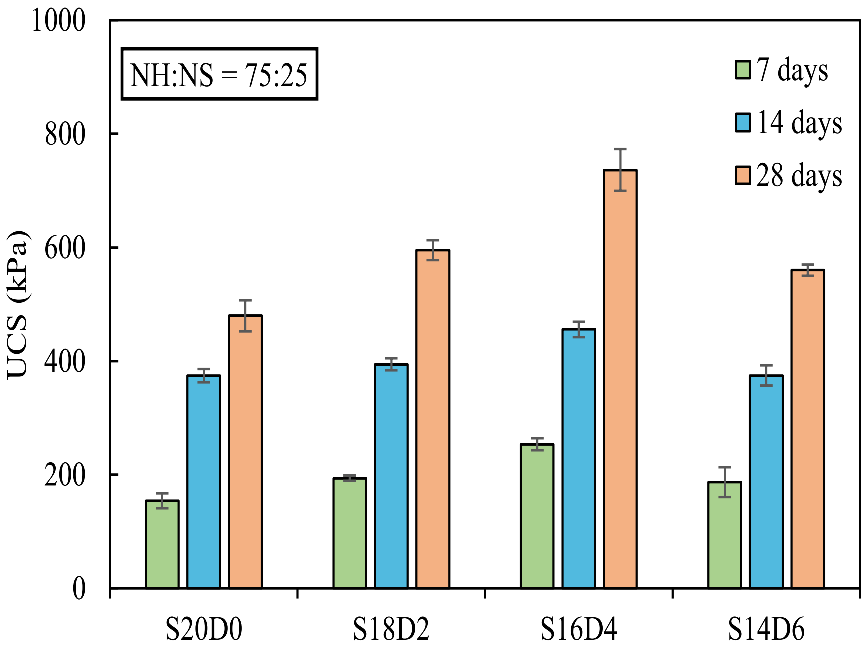
1000
800
600
400
200
0
UCS (kPa)
NH:NS = 75:25
7 days
14 days
28 days
S20D0
S18D2
S16D4
S14D6

(b)

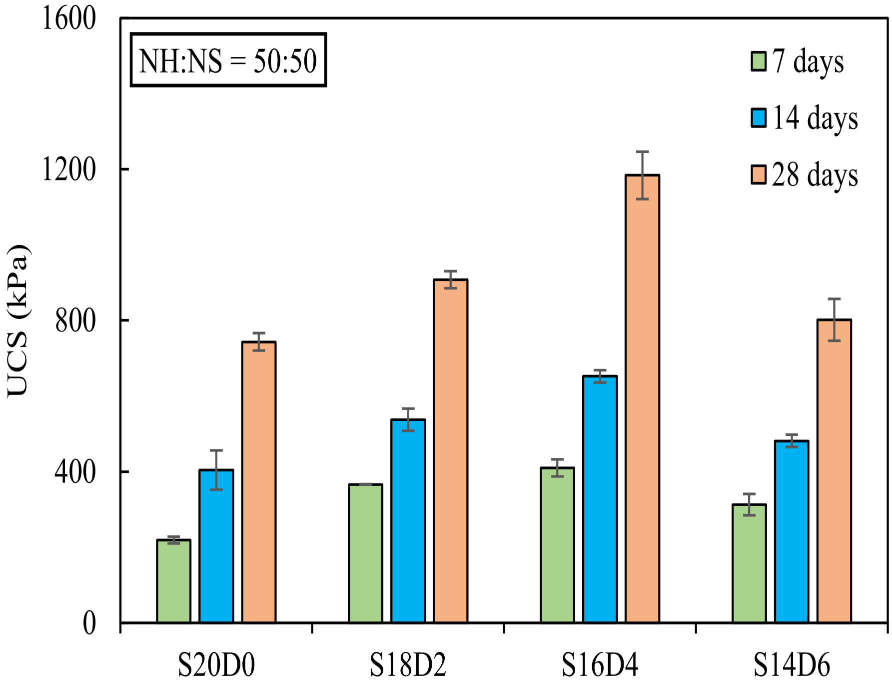
1600
1200
800
400
0
UCS (kPa)
NH:NS = 50:50
7 days
14 days
28 days
S20D0
S18D2
S16D4
S14D6

(c)

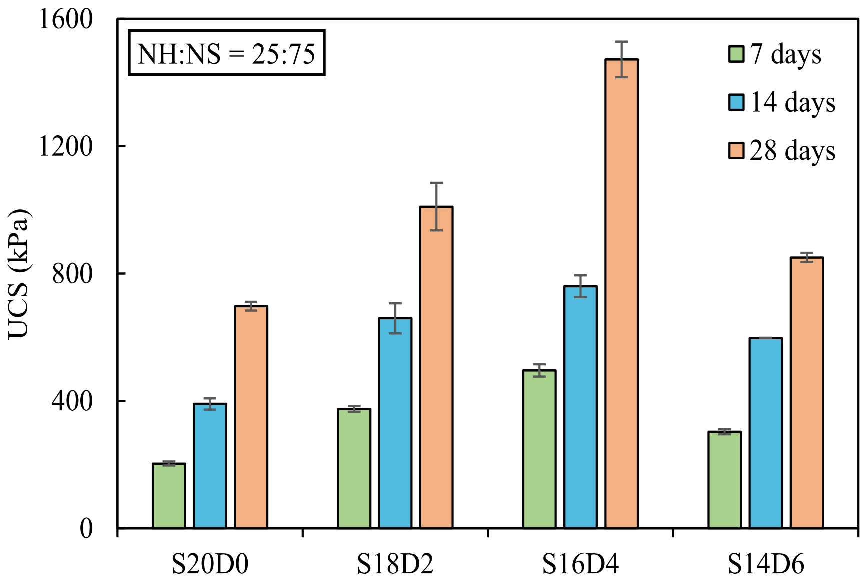

(d)

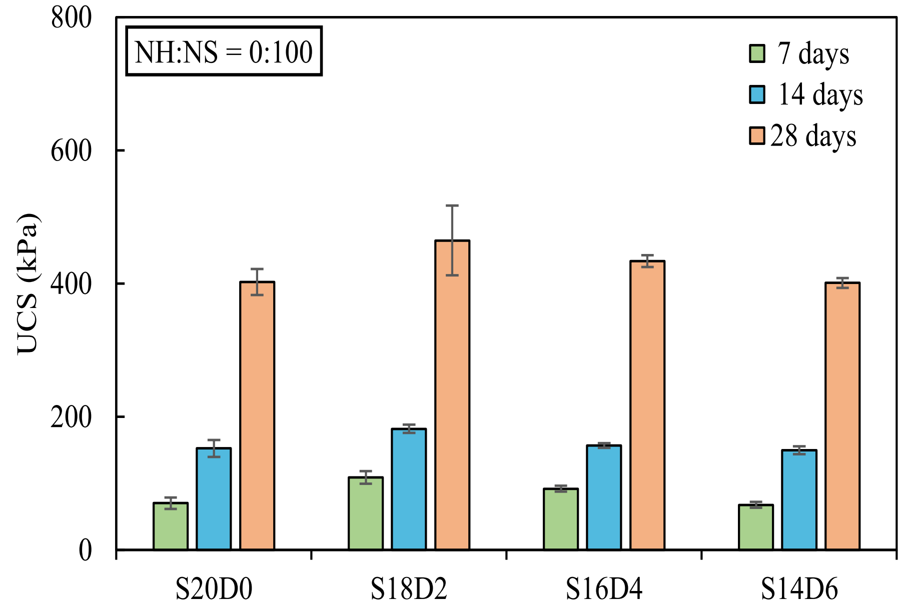

(e)

Fig. 4.2 Effect of GGBS and dolomite content on the compressive strength development for different mass ratios of NH and NS after 7, 14, and 28 days of curing period: (a)100:0, (b) 75:25; (c) 50:50, (d) 25:75, and (e) 0:100.

The effect of adding the dolomite powder to GGBS (with 20% precursor content) with an NH:NS ratio of 25:75 on the compressive strength of kaolin clay is presented in Fig. 4.3. The addition of dolomite has a positive effect on the geopolymerization process. On comparing the compressive strength of GGBS and dolomite stabilized clay with OPC stabilized clay, it was found that with the addition of dolomite up to 4%, the compressive strength significantly improved and was more than the cement-treated specimens. It can be seen that the compressive strength of all the GGBS and dolomite-based geopolymer specimens is more than the OPC 10 (control 2) specimens for all curing periods. Also, the strength of the NH25NS75S16D4 specimen was higher than that of the OPC20 (Control 3) specimen for all the curing periods. The strength of the NH25NS75S16D4 specimen was 26.30%, 32.59%, and 38.35% higher than the OPC20 specimen for the 7, 14, and 28 days curing period, respectively.

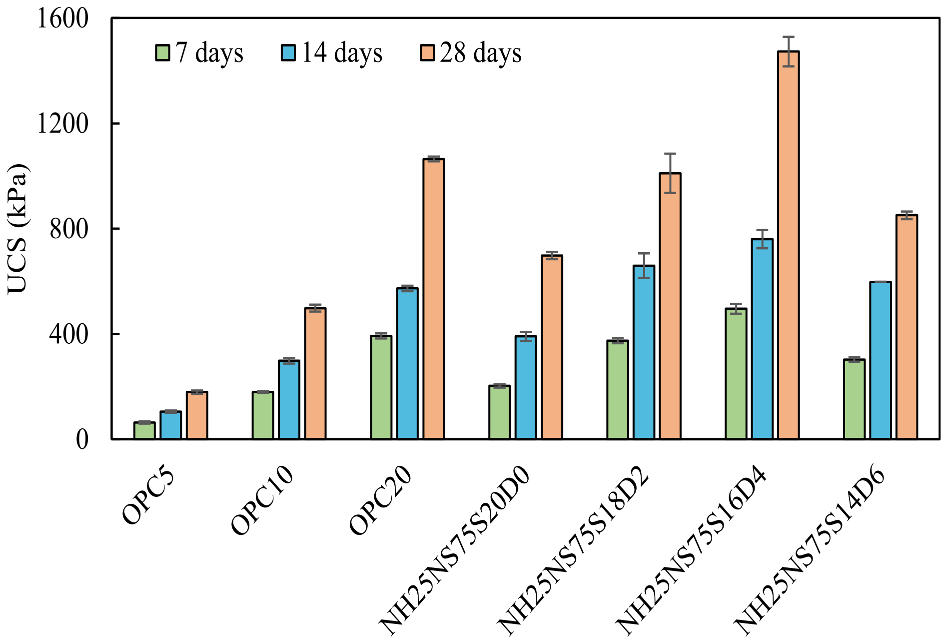

Fig. 4.3 UCS of the geopolymer stabilized specimen stabilized with NH:NS ratio of 25:75 and different ratios of GGBS and dolomite compared with the OPC stabilized specimens after 7, 14, and 28 days of curing period.

4.3.1.3 Effect of NH:NS ratio

The mass ratio of NH and NS plays a significant role and has the highest impact on the compressive strength of GGBS and dolomite-based geopolymer-treated clay. Fig.

4.4 shows the effect of the NH:NS mass ratio on the 7, 14, and 28 days compressive strength of the different ratios of GGBS and dolomite-based geopolymer stabilized clay. NH acts as a dissolvent that mainly dissolves silica and alumina in the clay and precursor, and NS acts as a binding agent in the geopolymerization process (Arulrajah et al. 2018). It can be seen that with the addition of NS, the compressive strength of all the specimens increases significantly for all GGBS and dolomite ratios. Also, previous studies have reported that the increase in NS mass ratio in NH:NS ratio causes the increase in strength, and maximum impact was obtained with 70-80% of NS mass ratio (Hardjito et al. 2005; Phetchuay et al. 2016; Sukmak et al. 2019; Suksiripattanapong et al. 2022; Zhou et al. 2021). More reaction product is formed at this mass ratio, favoring the geopolymerization process. At an NH mass ratio of 100%, there is an adequate amount of $[OH]^-$ ions, but there is a lack of $[SiO_4]^{4-}$ in the matrix to react with Ca^{2+} to form C-A-S-H gel. Using a 100% NS mass ratio in the geopolymerization processes leads to an increase in the amount of $[SiO_4]^{4-}$ and a decrease in the alkalinity in the matrix. On increasing the mass of NH in the NH:NS ratio from 100:0 to 25:75, there is an increasing trend in the strength of all the specimens. However, with the use of GGBS only in the specimens, the strength of NH:NS ratio of 50:50 and 25:75 is almost similar, as shown in Fig. 4.4(a). With the addition of dolomite in the mix, there is an increase in the Ca^{2+} ions, which reacts with the $[SiO_4]^{4-}$ in the system and results in maximum strength at an adequate NH: NS mass ratio of 25:75.

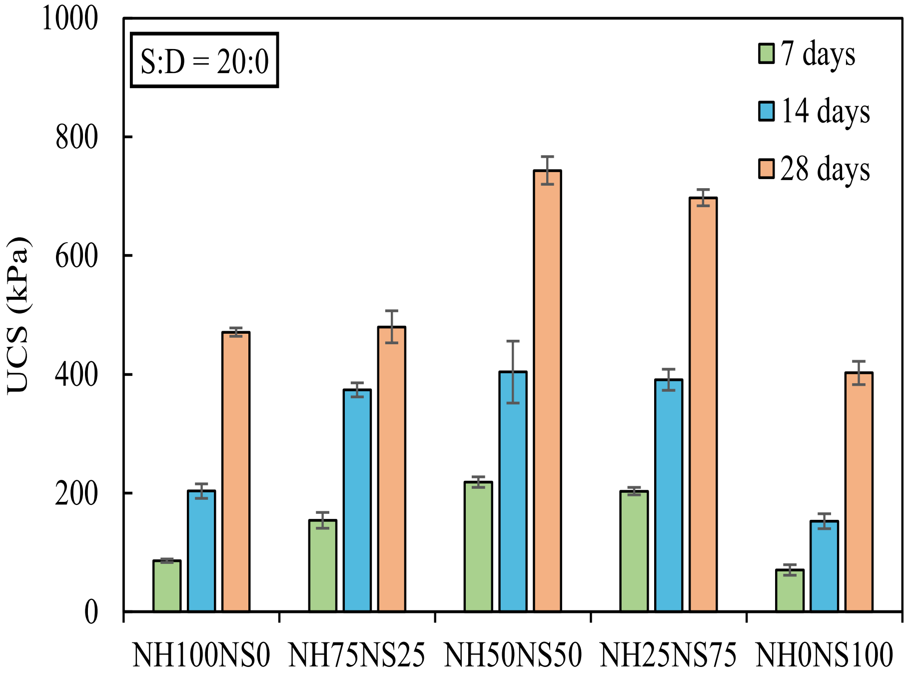
1000
800
600
400
200
0
UCS (kPa)
S:D = 20:0
7 days
14 days
28 days
NH100NS0
NH75NS25
NH50NS50
NH25NS75
NH0NS100

(a)

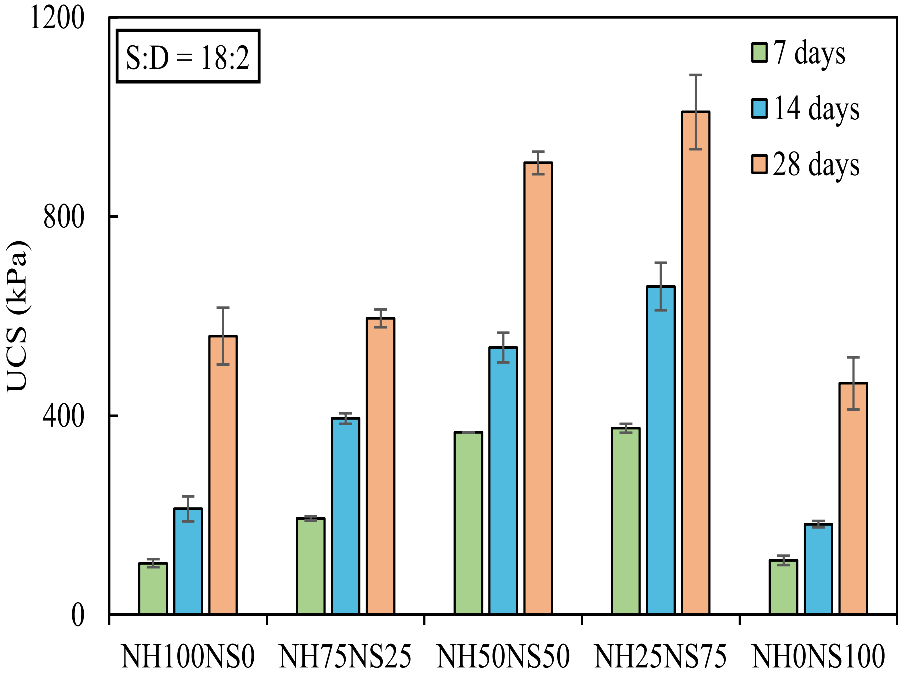
1200
800
400
0
UCS (kPa)
S:D = 18:2
7 days
14 days
28 days
NH100NS0
NH75NS25
NH50NS50
NH25NS75
NH0NS100

(b)

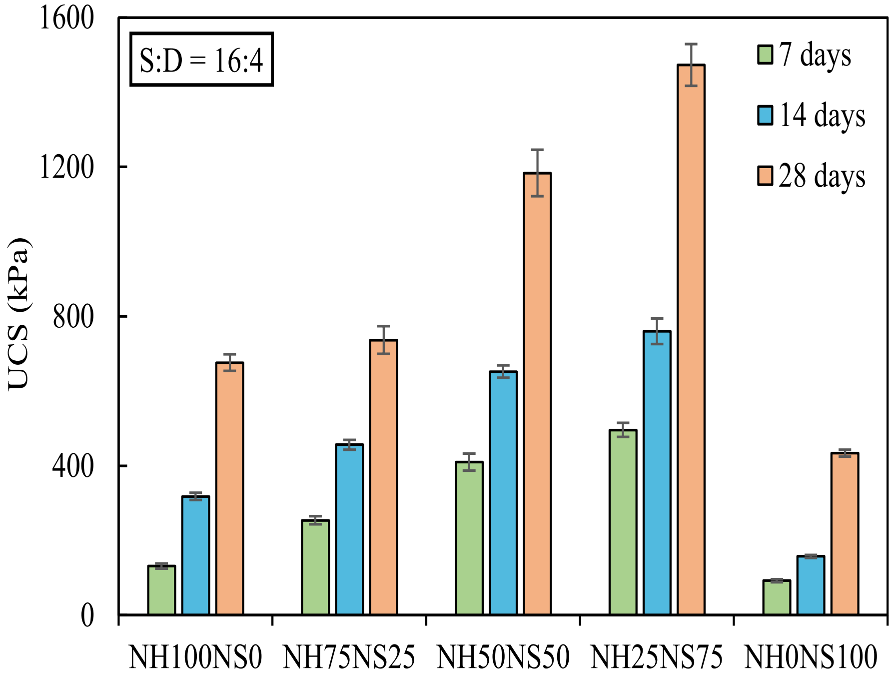

(c)

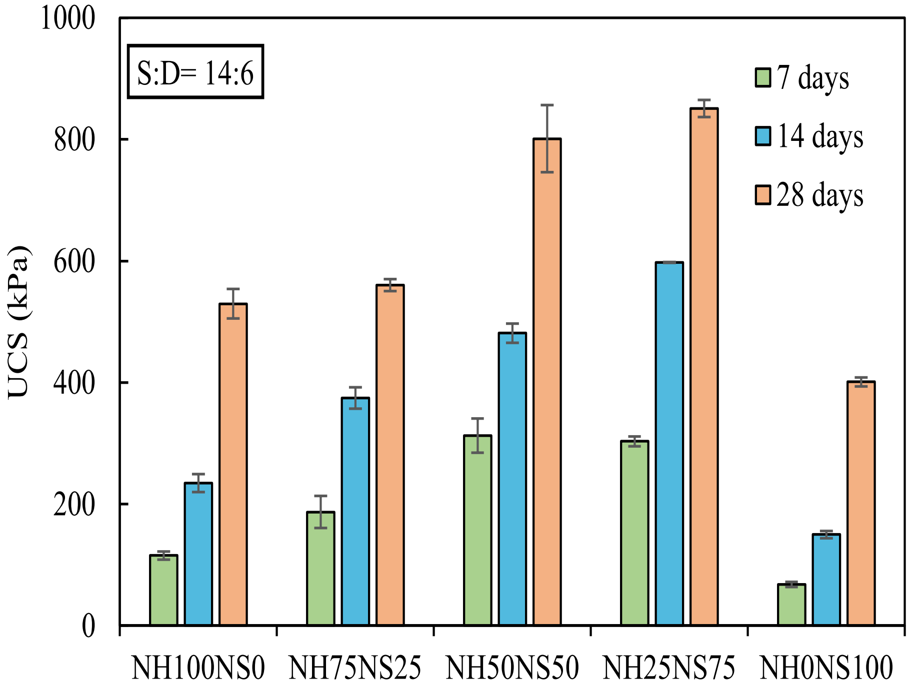

(d)

Fig. 4.4 Effect of NH and NS mass ratio on the compressive strength development for different ratios of the GGBS and dolomite under 7, 14, and 28 days of curing period: (a) S:D=20:0, (b) S:D=18:2, (c) S:D=16:4, and (d) S:D=14:6.

The UCS test results after 28 days of curing for various ratios of NH and NS, and GGBS and dolomite are presented in Fig. 4.5. It can be seen that for all the NH:NS ratios, there is an increase in UCS value with an increase in NS up to an optimum content, and above that, decreases in UCS values were observed. It is also evident that the optimum NH:NS ratio depends on the precursor. With the decrease in the NH:NS ratio from 100:0 to 50:50, there is an increase in the UCS value for GGBS-treated specimens, and the further decrease in the NH:NS ratio leads to a reduction in the UCS value. However, the addition of dolomite with GGBS results in an increase in UCS up to an NH:NS ratio of 25:75. A relatively lower NH:NS ratio was beneficial to the strength development of GGBS and dolomite-treated specimens, whereas a higher ratio of NH:NS was beneficial to the GGBS treated specimens. In conclusion, the optimum NH:NS ratio at which maximum strength was obtained without adding dolomite is 50:50, and with the addition of dolomite, the optimum ratio is 75:25.

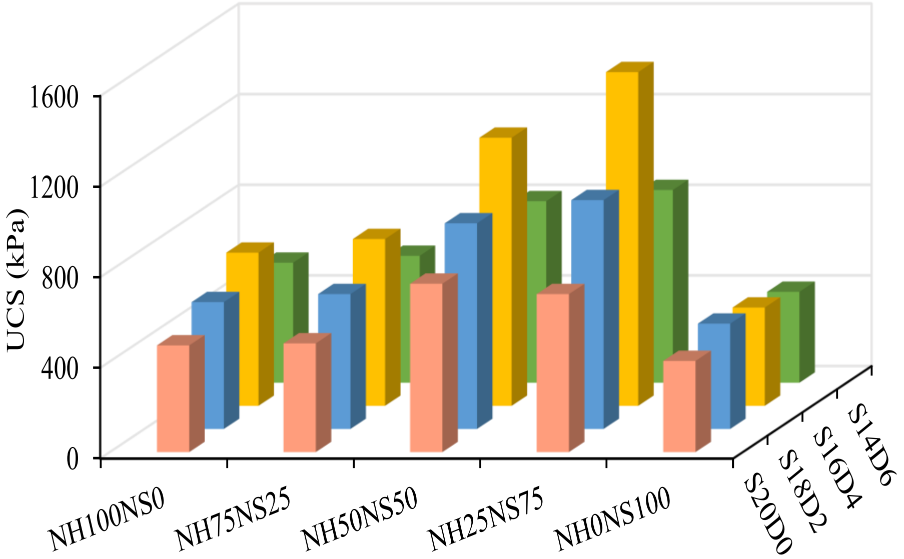

Fig. 4.5 Effect of NH and NS mass ratio and GGBS and dolomite content on the compressive strength development after 28 days of curing period.

4.3.1.4 Effect of curing time

Fig. 4.6 shows the effect of strength development of cement and geopolymer stabilized clay activated with NH:NS mass ratio of 25:75 over 7, 14, and 28 days curing time. The geopolymerization is a time-dependent process, i.e., the development of gel formation depends on the curing time. The strength of the OPC20 specimen is almost similar to the NH25NS75S16D4 specimen over 7 days curing period. The rate of increase in UCS value from 7 to 14 days for OPC20 and NH25NS75S16D4 specimens was 46.07% and 53.34%, respectively. After 28 days of curing, the OPC20 specimen exhibited an increase of 85.7% in compressive strength compared to 14 days, whereas, for the NH25NS75S16D4 specimen, the increase in compressive strength was 93.8%. Therefore, it can be concluded that the strength gain rate of NH25NS75S16D4 was higher than OPC20 for all curing times.

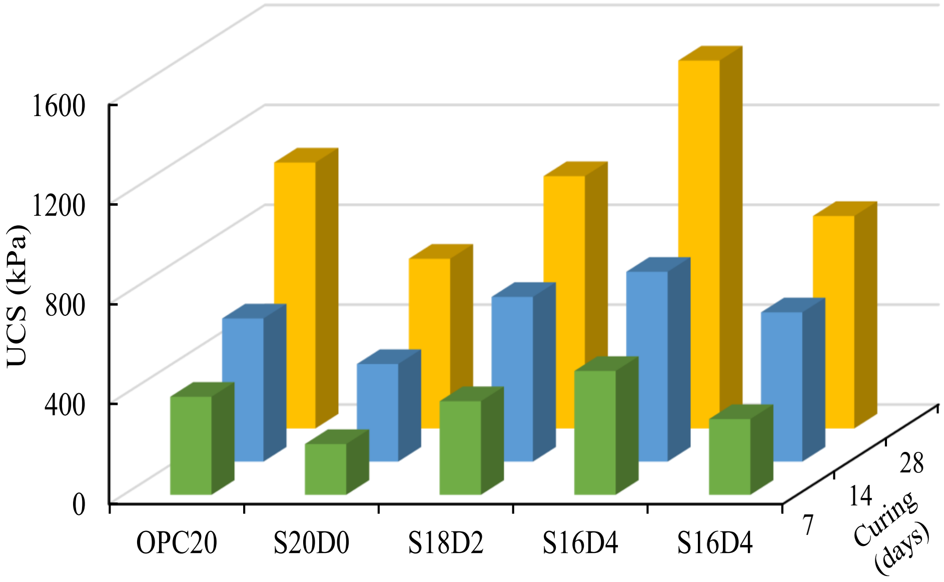

Fig. 4.6 Effect of curing period on the compressive strength development of GGBS and dolomite stabilized specimens.

Typical UCS development with curing time for the geopolymer stabilized kaolin clay with different S:D ratios and NH:NS ratios is shown in Fig. 4.7. A relationship was developed at any curing period (UCS_D) and at a curing time of 28 days (UCS_{28}) to predict the strength development over curing time (days). For the normalized analysis, the UCS values of the mix designs were normalized based on their corresponding 28 days UCS values, as previously done by (Horpibulsuk et al. 2011; Phetchuay et al. 2016; Yaghoubi et al. 2018). Fig. 4.7 shows the normalized (UCS_D/UCS_{28}) value with the curing time. An equation was developed with a high correlation coefficient (Eq. 1). The strength can be predicted using the above-proposed equation at a specific curing time between 7 and 28 days. This equation is similar to that reported by (Horpibulsuk et al. 2011) for soft Bangkok clay stabilized using OPC, fly ash, and biomass ash admixtures, (Phetchuay et al. 2016) for Coode Island Silt soil using fly ash and CCR geopolymer admixtures, and (Yaghoubi et al. 2018) for Coode Island Silt soil stabilized using fly ash and slag geopolymer admixtures. It was found that the results reported in this study were relatively similar to the previously reported literature, with the difference due to different types of soil, types of precursors, and precursor contents used. However, results were similar, suggesting that the strength development was due to the same geopolymer reaction mechanism.

$$\boldsymbol{UCS_D/UCS_{28} = 0.509\ln(D) - 0.731} \qquad (1)$$

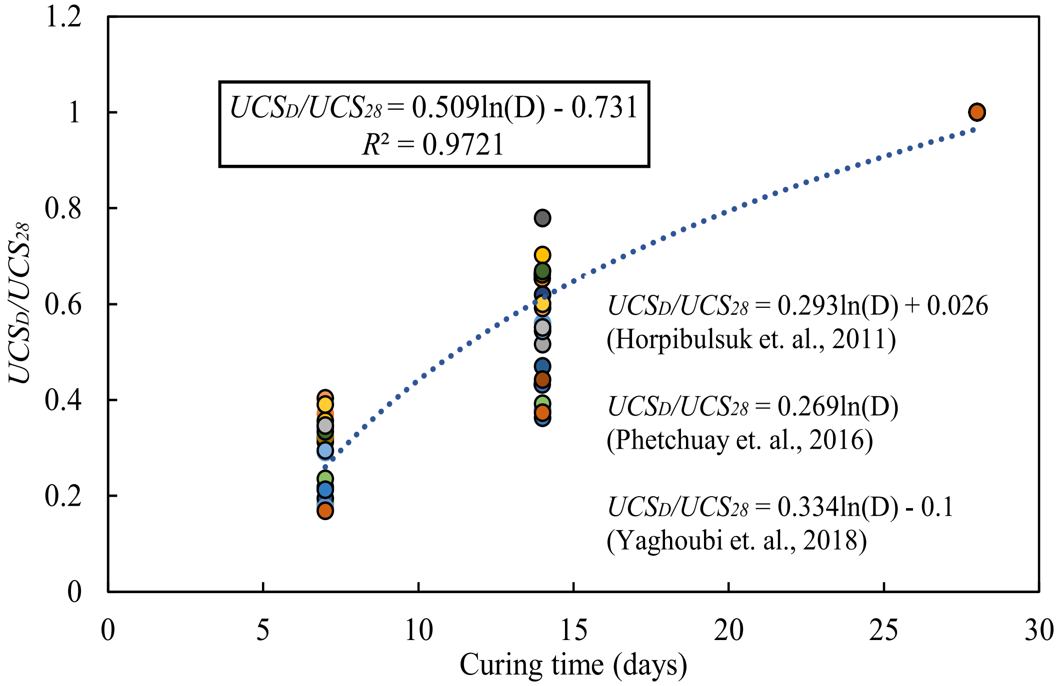

Fig. 4.7 Strength development with time for different NH and NS mass ratios, GGBS and dolomite, and their correlation.

4.3.1.5 Effect of water content of soft soil

The UCS values of the samples prepared with different water contents of 0.8LL, 1LL, and 1.2LL of kaolin clay cured at 27 °C for a curing period of 7, 14, and 28 days at a particular NaOH: Na_2SiO_3 ratio of 25:75 and L/P ratio of 1 is shown in Fig. 4.8 to illustrate the effect of different S:D ratio on the strength of the stabilized clay. The UCS value for all S:D ratios increases with curing time for all water contents. S and D-based geopolymer-stabilized kaolin clay showed the highest UCS when an S:D ratio of 16:4 was used. It can be explained by the geopolymer reaction, which occurs due to the dissolution of Si^{4+} and Al^{3+} ions from ground granulated blast furnace slag, Ca^{2+} ions from dolomite in NaOH and Na_2SiO_3 solution, and as a result formation of calcium aluminosilicate hydrate (C-A-S-H) and sodium aluminosilicate hydrate (N-A-S-H) gel which finally gives the cementitious product. Ca^{2+} from dolomite helps shorten the setting time and provides extra nucleation areas for precipitate formation, accelerating the geopolymerization process (Cristelo et al. 2011). On increasing the D replacement ratio in *S,* i.e., at an S:D ratio of 14:6, there is a decline in UCS value because of the excess formation of calcium hydroxide ($Ca(OH)_2$) crystals causing a negative effect on the strength development as it restrains the leaching of silica and alumina ions (Eun et al. 2010). From S:D ratio of 20:0 to of 16:4, increase in 28 days strength was 75.06%, 116.81%, and 141.89% for water content of 0.8LL, 1LL, and 1.2LL, respectively. Furthermore, on increasing the curing period from 7 to 28 days, the increase in strength of the S:D ratio of 16:4 is 70.82%, 67.29%, and 55.94% for the water content of 0.8LL, 1LL, and 1.2LL, respectively.

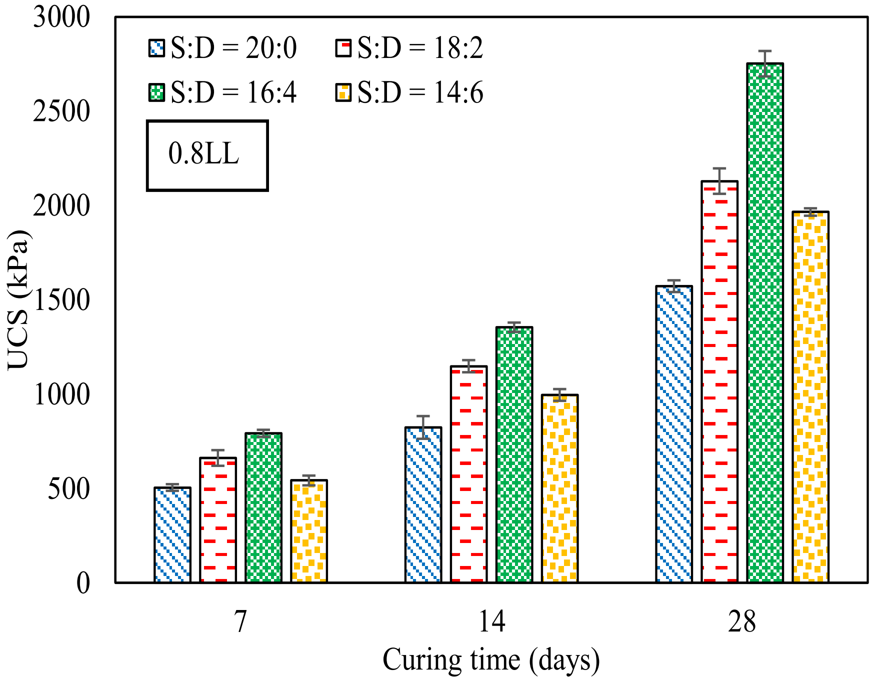

(a)

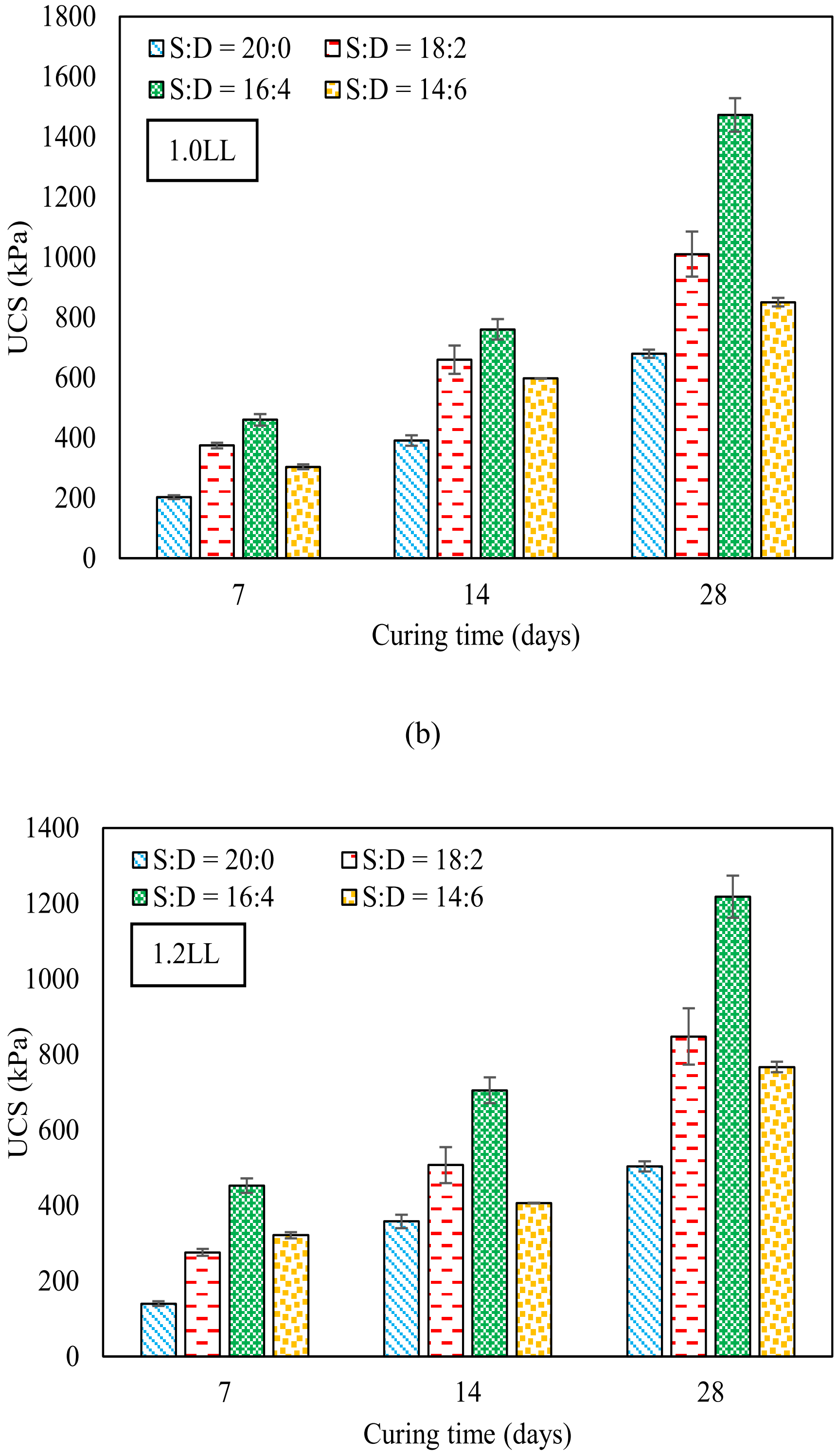

(b)

(c)

Fig. 4.8 Variation in strength with curing time for mixtures at various ratios of S and D and water content of (a) 0.8 LL, (b) 1 LL, and (c) 1.2 LL.

The variation of UCS of 28-day cured samples with a water content of kaolin clay for different mixtures of geopolymer and 20% cement is shown in Fig. 4.9. It was found that for all water contents, the strength of cement-improved kaolin clay is less than the strength of S:D based geopolymer with a ratio of 16:4. As water content of kaolin clay increases from 0.8LL to 1.2LL, UCS of the both geopolymer-stabilized as well as cement-stabilized kaolin clay decreases. This decreasing trend of UCS with water content can be explained as with the increase in water content, the alkalinity of the mixture decreases due to the dilution effect, and space between the soil particles increases, which reduces the friction and cohesion between the particles.

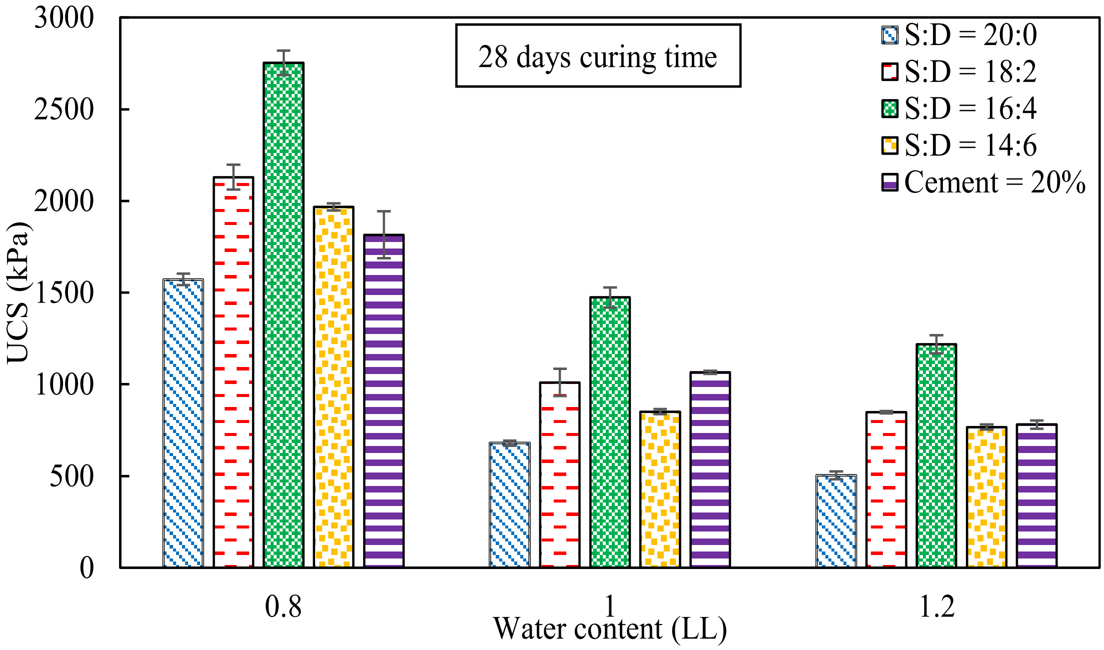

Fig. 4.9 Effect of water content on the 28 days UCS of geopolymer and cement-stabilized samples.

4.3.1.6 Effect of L/P ratio

Fig. 4.10 shows the effect of varying L/P ratio on 7-days, 14-days, and 28-days UCS of geopolymer-stabilized kaolin clay with an S:D ratio of 16:4 at a water content of 1LL. UCS increases with an increase in the L/P ratio, and maximum UCS values were obtained at L/P ratio of 1, which is the optimum L/P ratio for all curing times. With the increase in L/P ratio beyond 1, UCS decreases significantly. This could be due to the early formation of geopolymer products, which does not give enough time to S and D to react and restrains further reaction. Also, the replacement of Ca^{2+} ions is hindered due to excess Na^{+} ions in the sample, which forms a layer of ions with high thickness resulting in reduced cohesion between clay particles (Peng et al. 2019). Overall, an S:D ratio of 16:4 with an L/P ratio of 1 was the optimum mix for higher water contents from 0.8LL to 1.2LL.

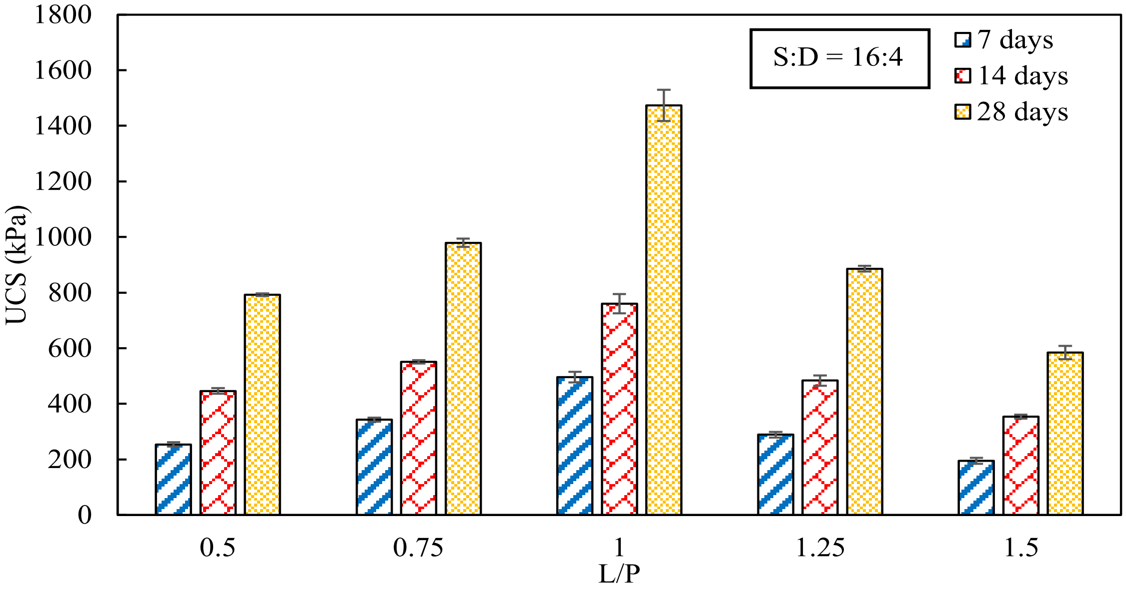

Fig. 4.10 Effect of L/P ratio on UCS of 7-days, 14-days, and 28-days cured samples.

4.3.2 Effect of alkali activator and GGBS-dolomite on the pH value

The pH value of all the mix proportions is presented in Fig. 4.11. The pH of kaolin clay was 7.51, showing the need for activation, as the minimum pH required to maintain the geopolymer reaction was 11 (Garcia-Lodeiro et al. 2015). The strength development of the geopolymer stabilized soil is mainly influenced by their pH value. An increase in pH in the geopolymerization process indicates the dissolution and condensation reaction as the OH- ions in the alkali activator solution induce hydrolysis of aluminate and silicate in the soil and precursor (Abdullah et al. 2019a). To determine whether the geopolymer clay treatment in this study compiles with the pH level of > 11, a pH test was performed on all the specimens after 7, 14, and 28 days of curing. The results show that adding geopolymer increases the pH level for all the mix proportions. The minimum increase in pH was found in the NS-treated specimens that ranged between 11.21 and 11.52 after 7 days of the curing period. The low pH and poor strength could be the absence of OH^- ions in the alkali activator. Also, adding dolomite positively affected the pH level of the geopolymer-stabilized clay. The maximum pH value of 12.83 was recorded for the NH25NS75S16D4 specimen. The results are consistent with the UCS test and support that adding dolomite helps in strength development.

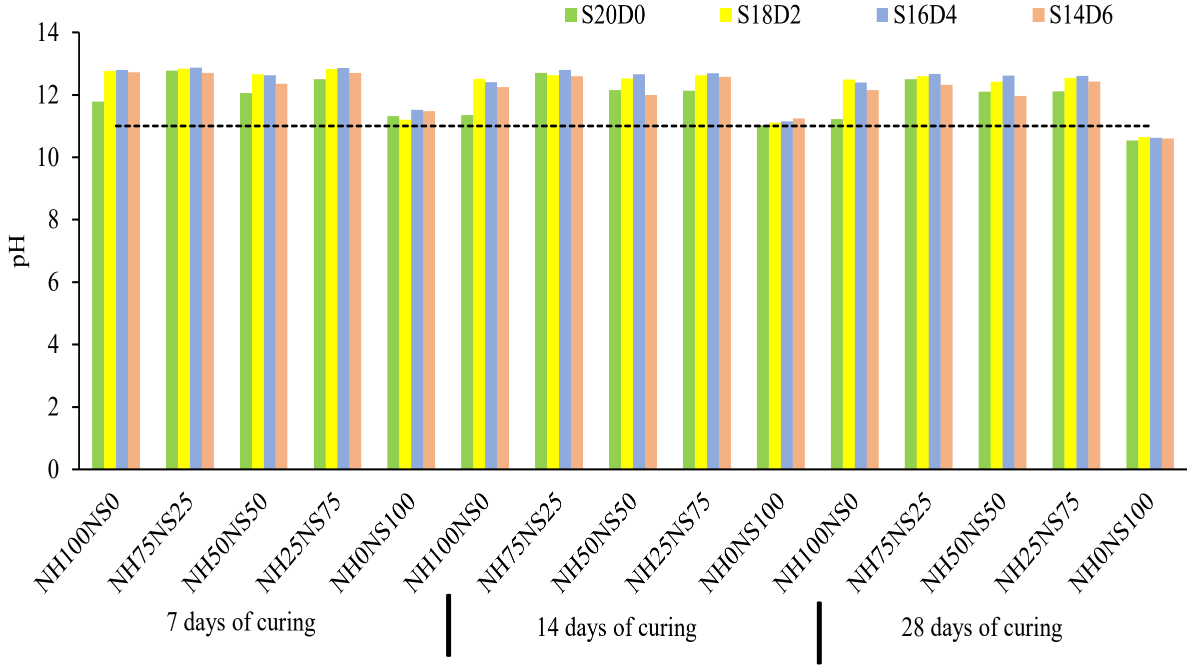

Fig. 4.11 pH of all the mix proportions of the geopolymer for stabilizing kaolin clay after 7, 14, and 28 days of curing period.

4.3.3 Undrained shear response of geopolymer treated soft soil under static loading

A series of CU triaxial tests on the optimum mix proportion of geopolymer-stabilized kaolin clay obtained using UCS test results were conducted to investigate the shearing behavior and shear strength parameters of GGBS and dolomite for soil stabilization. Tests were performed on the 28 days cured samples with varying S and D content, i.e., S20D0, S18D2, S16D4, and S14D6, and constant NH and NS content, i.e., NH25NS75 under confining pressures (CP) of 100, 200, and 300 kPa. Fig. 4.12 shows the deviator stress-axial strain and corresponding excess pore water pressure-axial strain responses determined from the CU static triaxial test with varying GGBS and dolomite content under different confining pressures. The specimens tested under higher confining pressure failed with more significant deviatoric stress and strain, which shows that confining pressure contributed to a rise in residual stress. Fig. 4.12(a) shows that in the case of GGBS (S20D0) stabilized clay, the deviator stress increases monotonically with an increase in strain, and a peak was obtained at low strain followed by post-peak gradual strain softening behavior. With the addition of dolomite with GGBS, more prominent stiffer behavior with comparatively lower strain (i.e., higher deviatoric stress and low axial strain) from S20D0 was observed, and the post-peak strain softening (brittle) response was more significant, as shown in Fig. 4.12(b), (c), and (d). Specimens treated with GGBS and dolomite-based geopolymer likely possess an increase in a cementitious bond due to the formation of calcium aluminosilicate hydrate (C-A-S-H) gel along with (N-A-S-H) gel, which can be responsible for the high undrained shear response at low strain before yielding in the initial loading stage [79,85]. Further loading resulted in stress taken by the destructed soil matrix and broken cementitious bond. (Coop and Atkinson 1993), (Miura et al. 2001), and (Horpibulsuk et al. 2005) have explained this failure mechanism for cement-treated soil. (Abdullah et al. 2019b) found that this behavior was consistent for geopolymer-treated soils. At all confining pressures, the clay stabilized with S16D4 displayed much greater deviator stresses, nearly twice that of clay stabilized with S20D0. Fig. 4.12(c) shows that the specimens stabilized with S16D4 precursor; the increase in confining pressure helped increase the yield stress from 1.07 MPa to 1.47 MPa. The increase in confining pressure causes the rearrangement of the cemented clay clusters and an increase in friction, resulting in an increase in deviator stress (Horpibulsuk et al. 2004).

For all the specimens, the negative pore pressure was obtained during shearing, indicating the dilative behavior as presented in Fig. 4.12. Also, the developed excess pore water pressure increases with an increase in confining pressure. Larger volumetric strain was typically correlated with higher confining pressure, and greater dilatation was typically correlated with lower confining pressure (Yaghoubi et al. 2018). To better understand the undrained shear behavior of the GGBS and dolomite-stabilized kaolin clay, a comparison of normalized peak stress (i.e., stress ratio defined as the ratio of peak stress and confining pressure) with confining pressure was done, as shown in Fig. 4.13. The specimens treated with S16D4 precursor showed a higher stress ratio, which tended to decrease with an increase in confining pressure. The rise in the stress ratio of the S16D4 precursor at a lower confining pressure of 100 kPa signifies a rise in the cementation bond to the ultimate peak stress ratio. A relatively small influence on the stress ratio was seen at confining pressures of 200 and 300 kPa compared to confining pressures of 100 kPa. This result could be explained by de-structuring the cemented clay clusters under greater confining pressures before shearing (Zhang et al. 2023). The secant modulus of the specimens also exhibited a progressive increase due to the increased confining pressure, as shown in Fig. 4.14, and the stiffness increases as the dolomite content rises to an optimum value.

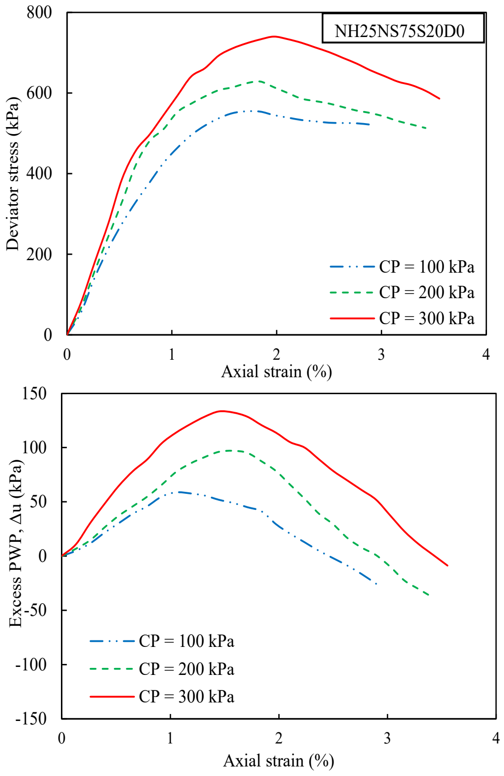
NH25NS75S20D0
Deviator stress (kPa)
0
200
400
600
800
0
1
2
3
4
Axial strain (%)
CP = 100 kPa
CP = 200 kPa
CP = 300 kPa
Excess PWP, Δu (kPa)
150
100
50
0
-50
-100
-150
0
1
2
3
4
Axial strain (%)
CP = 100 kPa
CP = 200 kPa
CP = 300 kPa

(a)

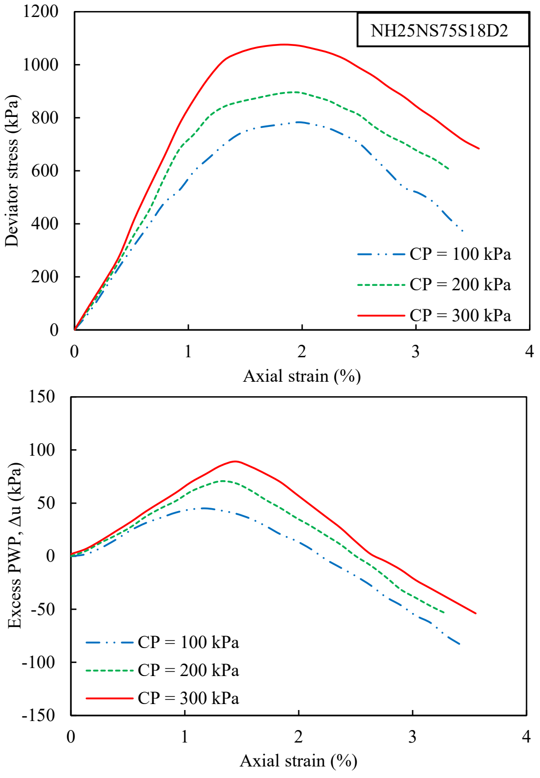
NH25NS75S18D2
Deviator stress (kPa)
0
200
400
600
800
1000
1200
0
1
2
3
4
Axial strain (%)
CP = 100 kPa
CP = 200 kPa
CP = 300 kPa
Excess PWP, Δu (kPa)
150
100
50
0
-50
-100
-150
0
1
2
3
4
Axial strain (%)
CP = 100 kPa
CP = 200 kPa
CP = 300 kPa

(b)

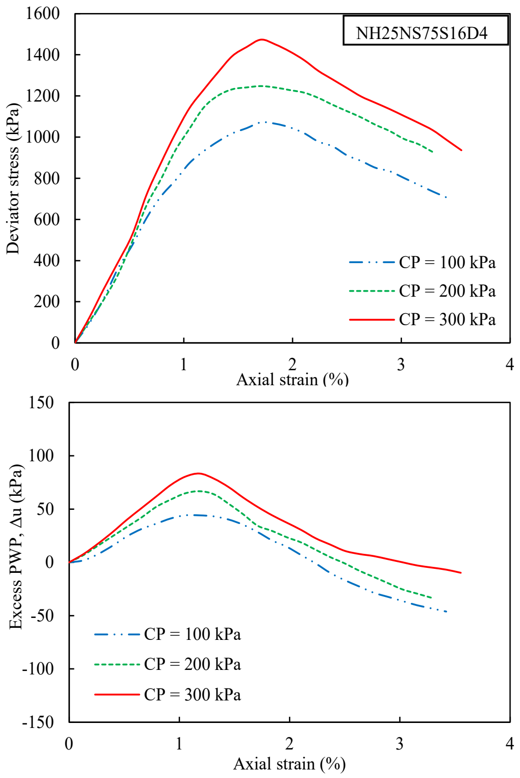
NH25NS75S16D4
Deviator stress (kPa)
0
200
400
600
800
1000
1200
1400
1600
0
1
2
3
4
Axial strain (%)
CP = 100 kPa
CP = 200 kPa
CP = 300 kPa
Excess PWP, Δu (kPa)
150
100
50
0
-50
-100
-150
0
1
2
3
4
Axial strain (%)
CP = 100 kPa
CP = 200 kPa
CP = 300 kPa

(c)

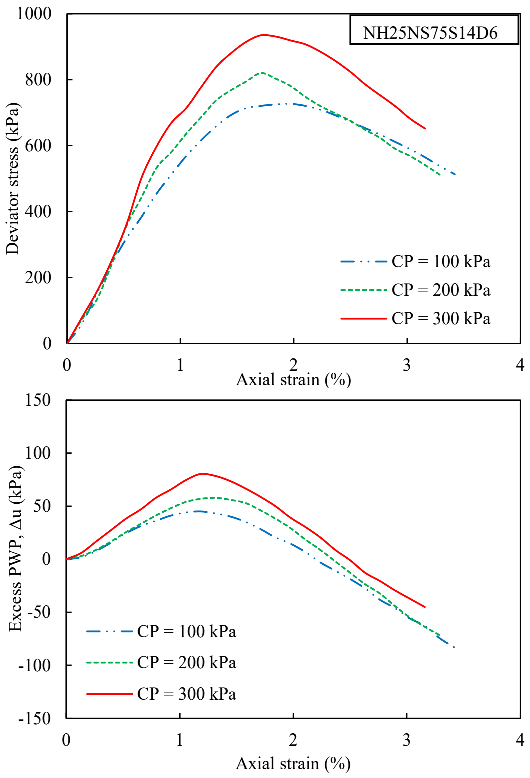
NH25NS75S14D6
Deviator stress (kPa)
0
200
400
600
800
1000
0
1
2
3
4
Axial strain (%)
CP = 100 kPa
CP = 200 kPa
CP = 300 kPa
Excess PWP, Δu (kPa)
150
100
50
0
-50
-100
-150
0
1
2
3
4
Axial strain (%)
CP = 100 kPa
CP = 200 kPa
CP = 300 kPa

(d)

Fig. 4.12 Typical CU triaxial test results of the specimens treated with different ratios of GGBS and dolomite at 100, 200, and 300 kPa confining pressures (cured for 28 days): (a) NH25NS75S20D0; (b) NH25NS75S18D2; (c) NH25NS75S16D4; (d) NH25NS75S14D6.

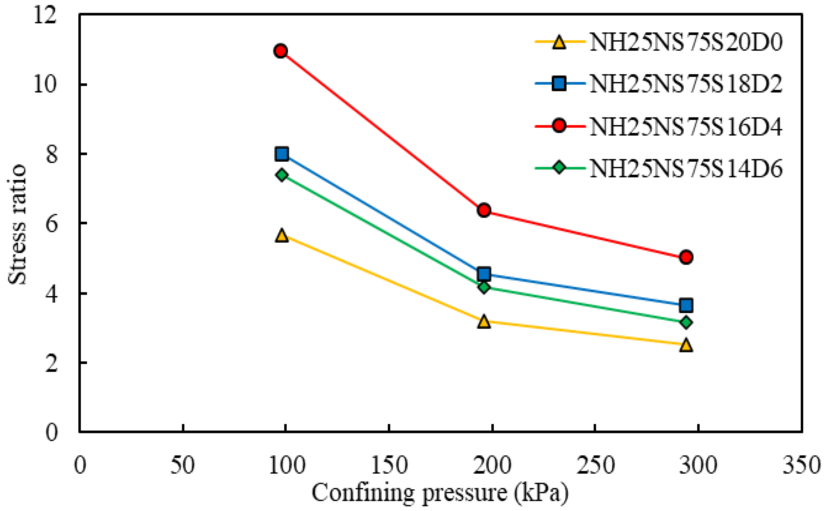

Fig. 4.13 Change in maximum stress ratio with an increase in confining pressure of the geopolymer-treated kaolin clay.

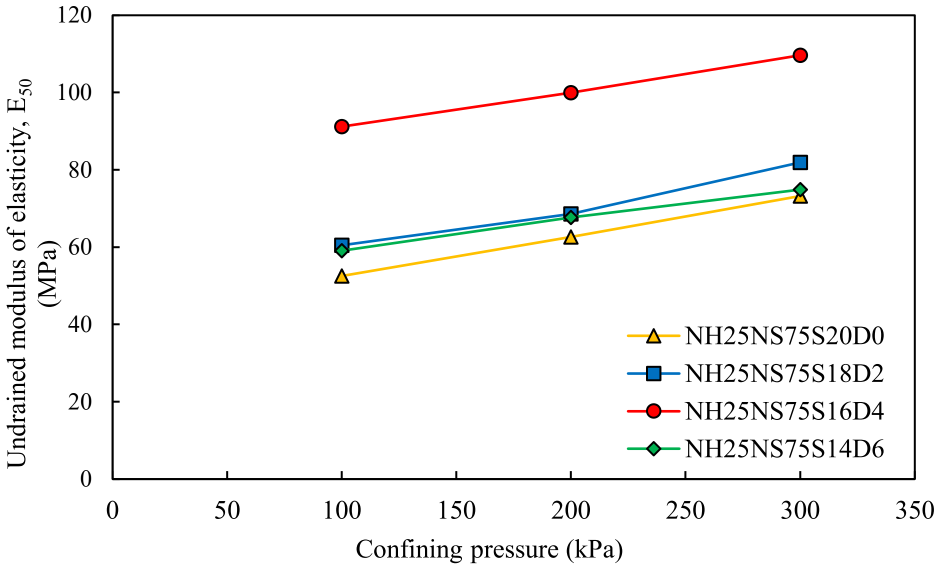

Fig. 4.14 Change in undrained modulus of elasticity (E_{50}) with an increase in confining pressure of the geopolymer-treated kaolin clay.

4.3.4 Undrained shear response of geopolymer treated soft soil under cyclic loading

The details of the cyclic triaxial testing system are shown in Table 4.2. Confining pressure of 50, 100, and 200 kPa were considered as these pressures are within the normal stress range for pavement subgrade (El Mohtar et al., 2013; Lang et al., 2020). Cyclic Stress Ratio of 0.5, 1.0, 1.5 and 2.0 corresponding to cyclic stress of 100, 200, 300, and 400 kPa, respectively, were taken considering the range of traffic load in the field (Leng et al. 2017). Furthermore, loading frequencies of 0.5, 1, 1.5, and 2 were selected considering the varied traffic loading conditions with different speeds (Sun et al., 1988; Tang et al., 2016; Min et al., 2022).

Table 4.2 Summary of the cyclic triaxial testing program.

Parameters	**Series**
Kaolin clay: precursor (P)	80:20
Precursor (S:D)	20:0, 18:2, 16:4, 14:6
NaOH: Na_2SiO_3 (L)	25:75
L/P	1
Curing time (days)	7,14,28
Confining pressure (kPa)	50, 100 and 200
Cyclic stress ratio (CSR)	0.5, 1.0, 1.5 and 2.0
Cyclic loading frequency (Hz)	0.5, 1.0, 1.5 and 2.0
Number of cyclic loading cycles (*N*)	10,000

Fig. 4.15 shows the typical results of the stress-controlled cyclic triaxial test on the geopolymer-stabilized kaolin clay specimens prepared at a water content of 1 LL, S:D ratio of 16:4, sheared at CSR of 1.0, $f = 1$ Hz, and $\sigma'_c = 100$ kPa.

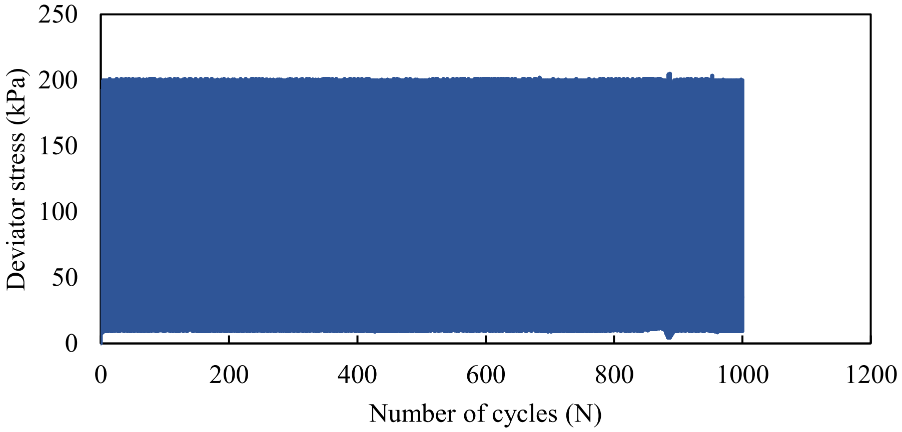
Deviator stress (kPa)
250
200
150
100
50
0
0
200
400
600
800
1000
1200
Number of cycles (N)

(a)

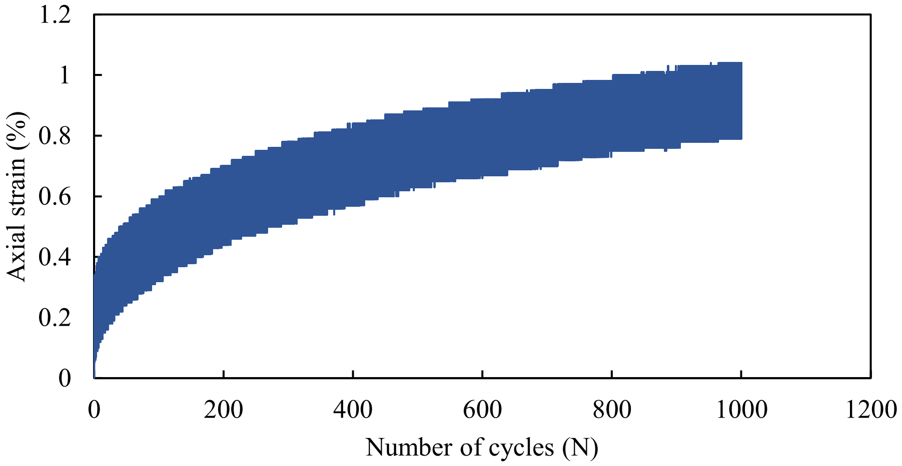
Axial strain (%)
1.2
1
0.8
0.6
0.4
0.2
0
0
200
400
600
800
1000
1200
Number of cycles (N)

(b)

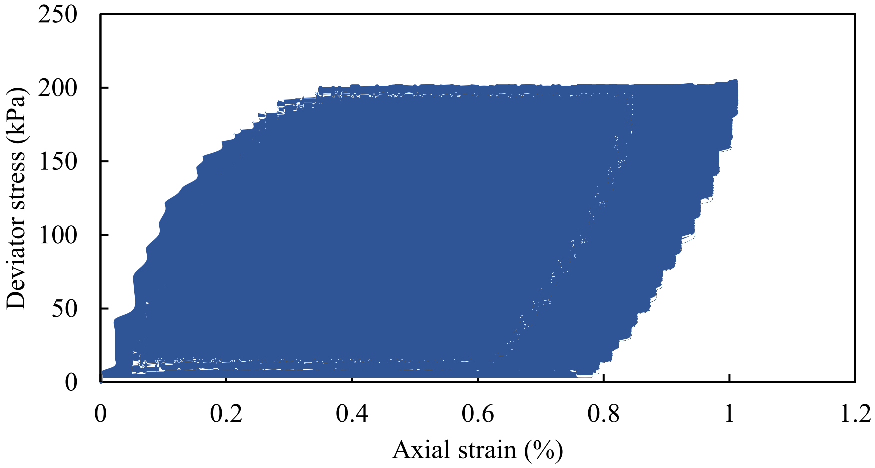
Deviator stress (kPa)
250
200
150
100
50
0
0
0.2
0.4
0.6
0.8
1
1.2
Axial strain (%)

(c)

Fig. 4.15 Typical results from the stress-controlled cyclic triaxial test of geopolymer-stabilized kaolin clay sample prepared with S:D ratio of 16:4 cured for 28 days at CSR of 1.0, f = 1 Hz, and σ'_c = 100 kPa: (a) Variation of deviatoric stress with N; (b) Variation of axial strain with N; (c) Variation of deviatoric stress with axial strain.

The deviatoric stress-axial strain hysteresis loop slope provides Young's modulus (E_{sec}), as shown in Fig. 4.16 (ASTM D3999, 2011). The dynamic shear modulus (G) is calculated using Poisson's ratio (ν) in the following equations-

$$G = \frac{E_{sec}}{2(1+\nu)} \tag{2}$$

The area of the hysteresis loop indicating the amount of energy dissipated due to cyclic loading is termed as damping ratio (λ), which is calculated using eq.

$$\lambda = \frac{A_{loop}}{(\pi A_T)} \tag{3}$$

Where A_{loop} is the area under hysteresis loop or the energy dissipated, and A_T is the area of the triangular portion or the stored strain energy during a loading cycle.

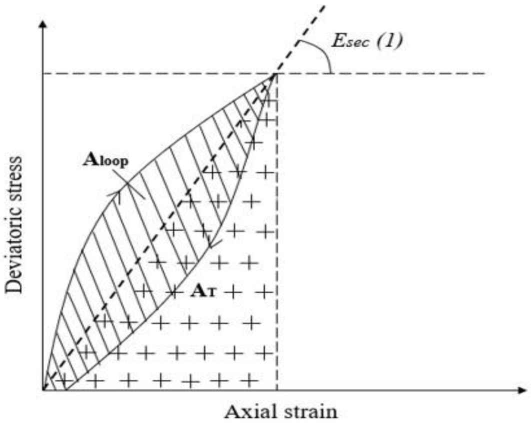

Fig. 4.16 Typical stress-strain hysteresis loop during cyclic triaxial testing program to estimate the dynamic parameters: G and λ.

4.3.4.1 Effect of change in S:D ratio

Fig. 4.17 shows the effect of S:D ratio on the axial strain for 10,000 cycles under a CSR of 1, CP of 100 kPa, and frequency of 1 Hz with a curing time of 28 days. Under the same number of cyclic loading cycles, higher axial strain is accumulated in an S:D ratio of 20:0. The strain response of S:D ratio of 18:2 and 14:6 is almost similar, and the accumulated strain is less than S:D ratio of 20:0. The samples stabilized with S:D ratio of 16:4 showed a stable trend and had less axial strain accumulation than other mixes for the same number of cycles. The reason could be optimum addition of D in the S increases the cementation bond between clay particles. The same results have been obtained in UCS test as S:D ratio of 16:4 has maximum shear strength. Fig.4.17(b) and (c) present the effect of S:D ratios on variation in geopolymer-stabilized kaolin clay's G and λ values. Higher G was obtained with the optimum addition of D content (S:D ratio = 16:4). However, further addition decreases G significantly under the same cyclic loading cycles. λ was found to increase for the first few cycles and finally tended to a stable value for all ratios of S and D. The cumulative strain of the samples increased, and λ hardly changed with an increase in N. Minimum damping was observed for the samples stabilized with S:D ratio of 16:4. The variation in degradation index (G/G_{max}) with shear strain for different ratios of S:D is shown in Fig. 4.17(d). The degradation index is the ratio of the dynamic shear modulus of the Nth cycle (G) to the initial cycle (G_{max}) (Seed and Idriss 1970). G/G_{max} curve is essentially a required parameter for cyclic loading conditions. Typically, G/G_{max} is less than 1, and a smaller G/G_{max} indicates higher degradation during cyclic loading (Subramaniam and Banerjee 2014). S:D ratio of 16:4 showed less stiffness degradation with shear strain than other ratios, which means that the degradation in the geopolymer bond during cyclic loading was less when the optimum geopolymer binder was used.

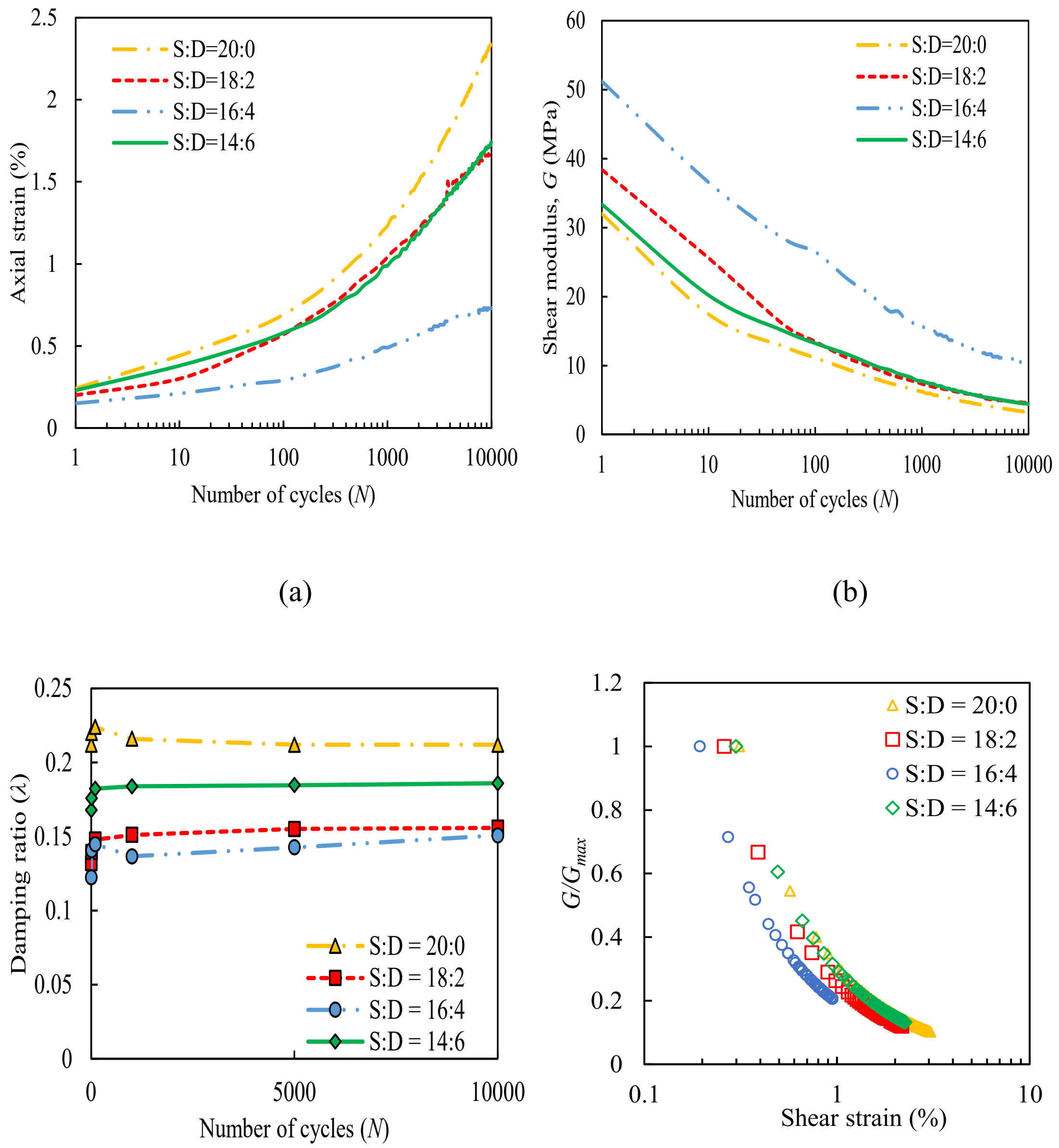

(a) (b)

(c) (d)

Fig. 4.17 Effect of different S:D ratios on the dynamic parameters (curing time = 28 days; CSR = 1; CP = 100 kPa; frequency = 1 Hz): (a) strain response with *N*; (b) variation of *G* with *N*; (c) variation of *λ* with *N*; (d) variation of G/G_{max} with shear strain.

4.3.4.2 Effect of CSR on stress-strain response and dynamic parameters

To analyze the effect of cyclic stress amplitude on the deformation behavior of geopolymer stabilized kaolin clay under constant CP, samples were subjected to cyclic stress ratio (CSR) of 0.5, 1, 1.5, and 2 corresponding to cyclic stress of 100, 200, 300, and 400 kPa respectively. Fig. 4.18(a) shows the strain response with the number of loading cycles at varying CSR to study the CSR threshold value. The results show that when CSR is less than or equal to 1, no prominent strain increment was observed with increased loading cycles. Also, the deformation increases rapidly within the first few cycles as most of the energy is absorbed during loading, resulting in a high amount of resilient strain and permanent strain. During the subsequent loading cycles, strain gets stabilized as the energy absorption rate gradually decreases with an increase in the number of cycles, and finally, stability is reached in the soil system (Pillai et al. 2011). However, as the CSR increases above 1, there is a greater rate of increase in strain accumulation until reaching the failure criteria. As the CSR is increased to 1.5, strain reaches 10% within 3700 cycles; at a CSR of 2, strain is 10% within 527 cycles.

At CSR = 0.5, the strain increases first at the beginning, then the strain is almost stabilized to 0.44 % at 10,000 cycles, and at this level of cyclic stress, the effect of cyclic loading is insignificant on the strain response. At CSR of 1, the strain is stabilized to 0.73% at 10,000 cycles. At a higher CSR value of 1.5, the axial strain increases gradually, and within 3700 cycles sample goes to a weaker state. As the CSR increases to the next higher value of 2, the strain of 10% is reached only within 527 cycles. This may be due to the rupture of the geopolymer cementation bond within the clay particles with increased cyclic stress amplitude.

The effect of CSR and the number of cycles (*N*) on the estimated value of *G* is shown in Fig. 4.18(b). As the plastic strain occurs in the first few loading cycles, logarithmic coordinates were used for N to observe the change in *G*. The repetitive loading for N number of cycles causes strain accumulation resulting in cyclic softening and the reduction of *G* for all levels of CSR. The decrease in *G* was observed with an increase in CSR due to the increase in strain level. For low CSR, within the first few cycles, *G* decreases quite rapidly, and then there is hardly any change up to 10,000 cycles as the change in strain is less after 1000 cycles. For CSR > 1, G decreases continuously, deteriorating the cementation bond between clay particles, and axial strain accumulates rapidly and reaches 10 % within a lesser number of cycles. The relationship between λ and shear strain with an increase in CSR is shown in Fig. 4.18(c). For a specific S:D ratio of geopolymer content and curing time, λ increases with an increase in CSR until a certain shear strain. As the shear strain increases above 1%, there is a significant reduction in λ at higher strain levels, similar to the trend obtained by (Kumar et al. 2018). Fig. 4.18(d) illustrates the variation of G/G_{max} with shear strain for different values of CSR. The degradation phenomenon represents the decrease in G with increases in loading cycles with an increase in CSR. A lower G/G_{max} with the increase in shear strain was observed when applied deviator stress was less, and an increase in deviatoric stress resulted in an increase in G/G_{max} with the shear strain. As most energy is absorbed within the first few loading cycles, an early degradation in the geopolymer bond was observed, causing a significant increase in plastic strain. The absorbed energy gradually decreases with the increase in loading cycles, resulting in a stable elastic deformation (Moses et al., 2003). G/G_{max} reduction with increasing shear strain confirms the softening behavior of geopolymer-stabilized kaolin clay at higher deviator stress amplitude.

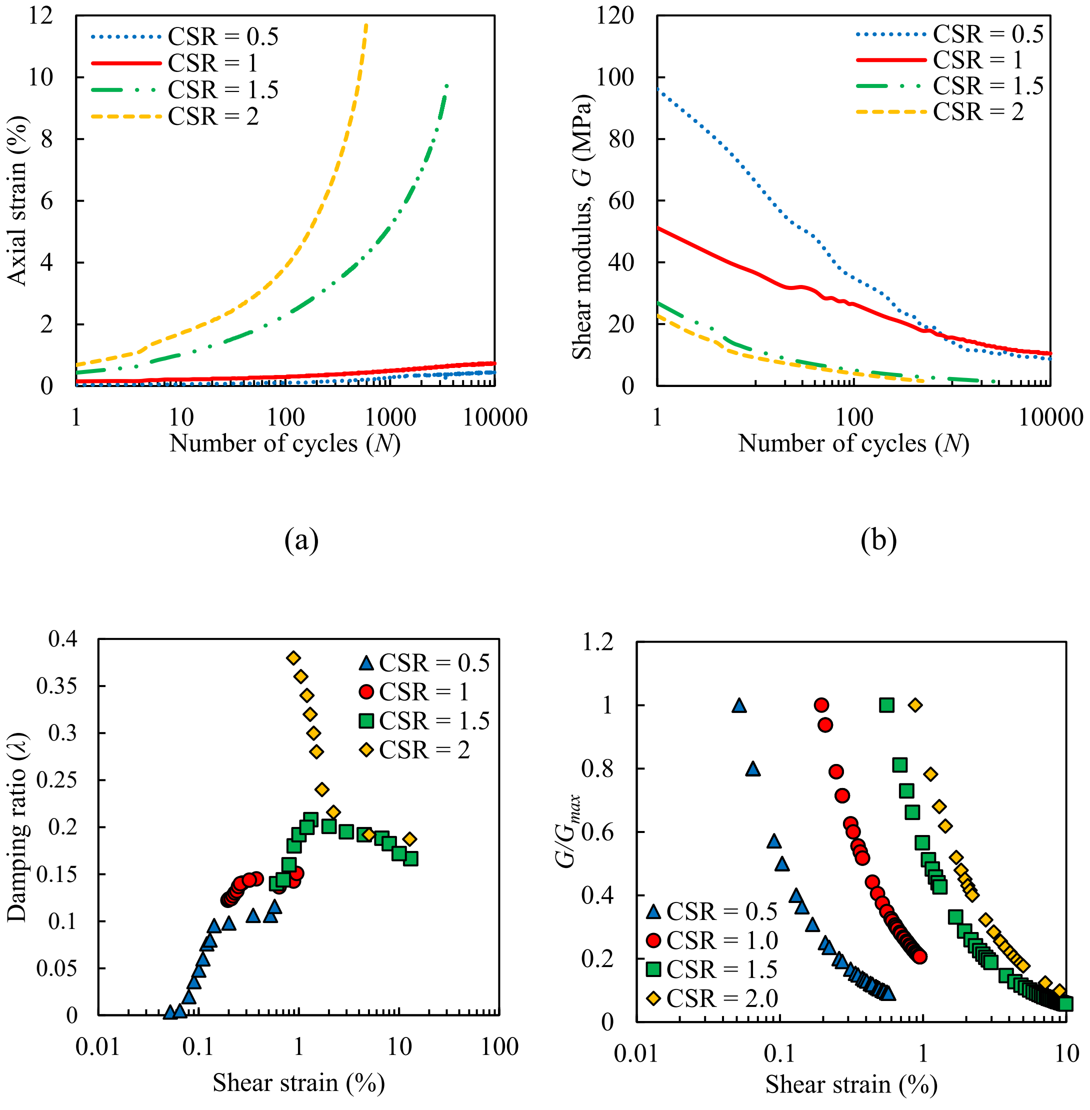

(a)

(b)

(c)

(d)

Fig. 4.18 Effect of CSR on the dynamic parameters (S:D = 16:4; curing time = 28 days; CP = 100 kPa; frequency = 1 Hz): (a) strain response with *N*; (b) variation of *G* with *N*; (c) variation of *λ* with shear strain; (d) variation of G/G_{max} with shear strain.

4.3.4.3 Effect of curing time

In the 7 days cured sample, axial strain dramatically accumulates within a few cycles until it reaches the failure criteria (Fig. 4.19(a)). However, when the geopolymer-stabilized sample is cured for 14 days, the strain response is more pronounced, and the failure criteria are reached within 2500 cycles. Furthermore, on curing the sample for a longer time (i.e., 28 days), axial strain accumulation is significantly less and stable up to 10,000 cycles. The dynamic shear modulus of the geopolymer-stabilized kaolin clay increases with an increase in curing time, and the rate of increase is much faster for curing time between 14 to 28 days (Fig. 4.19(b)). λ of 7 and 14 days cured samples increase at a faster rate until the sample fails. In contrast, λ of 28 days-cured samples is less and finally tends to stable value after a few loading cycles (Fig. 4.19(c)). G/G_{max} of 28 days cured sample is also less with shear strain as compared to 7 and 14 days cured samples, as shown in Fig. 4.19(d), which means that maximum stiffness is reached after 28 days of curing.

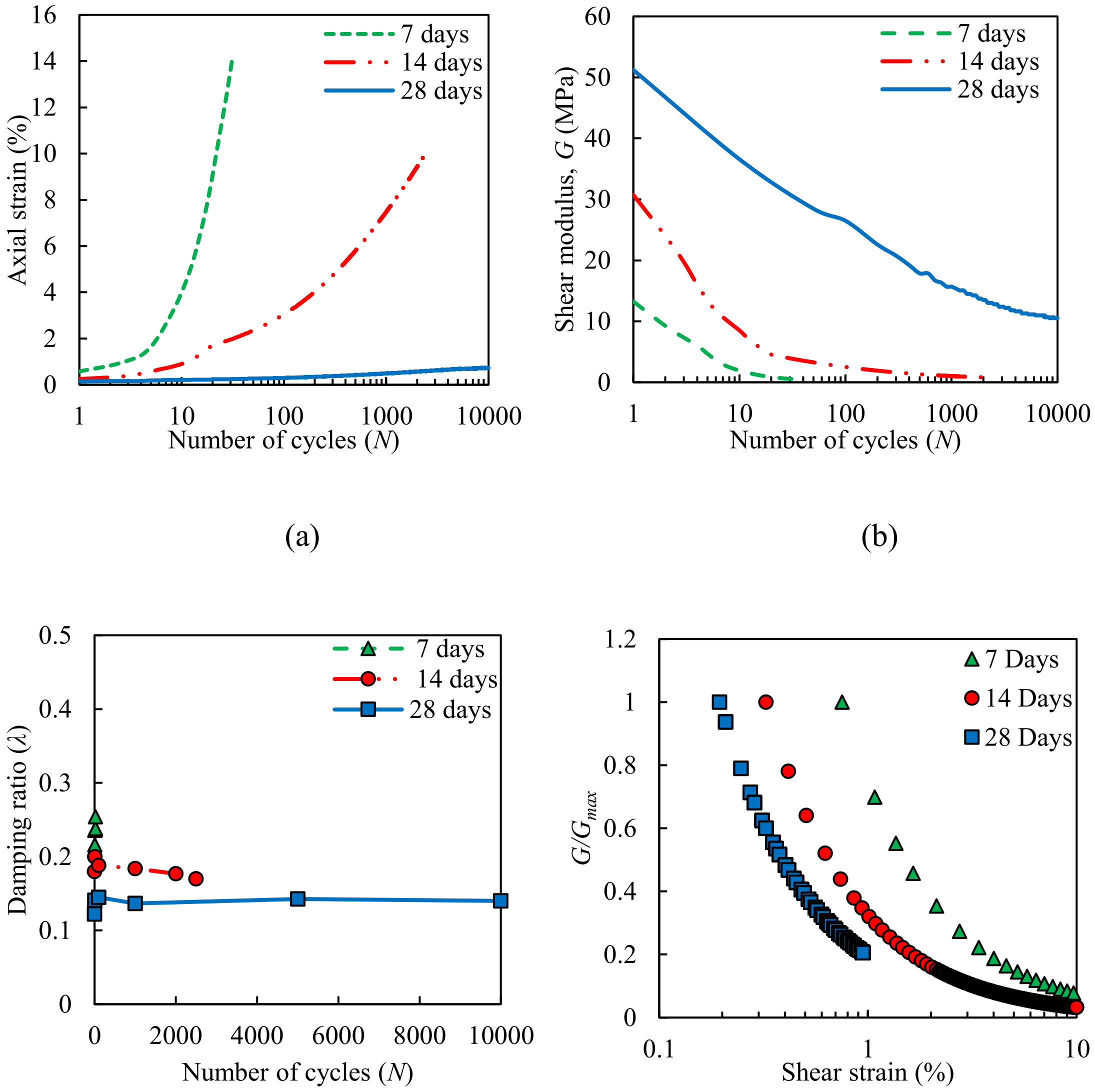

(a)

(b)

(c)

(d)

Fig. 4.19 Effect of curing period on the dynamic parameters (S:D = 16:4; CSR = 1; CP = 100 kPa; frequency = 1 Hz): (a) strain response with *N*; (b) variation of *G* with *N*; (c) variation of λ with *N*; (d) variation of G/G_{max} with shear strain.

4.3.4.4 Effect of change in frequency

As observed in Fig. 4.20(a), the accumulated axial strain increases with an increase in frequency. For a frequency of 0.5, the axial strain response is almost constant for 10,000 cycles, whereas, on increasing frequencies to 1 and 1.5, the strain response is stable for a few cycles and then increases at higher cycles. And on further increasing the frequency to 2, the accumulated strain continuously increases with the number of cycles. The main reason for this phenomenon is under higher cyclic-stress frequency, the applied stress energy increases within a certain period, causing a greater amount of energy loss and resulting in the degradation of the cementation bond of the geopolymer-stabilized kaolin clay (Moses et al., 2003). Fig. 4.20(b) reports that *G* decreases significantly with an increase in the cyclic-stress frequency from 0.5 to 1. *G* variation with the increase in *N* is almost the same for frequencies of 1 and 1.5, and on further increase in frequency, *G* decreases. G_{max} of the geopolymer stabilized sample under the frequency of 0.5 Hz is 50%, 60%, and 91% higher than the samples tested under frequencies of 1, 1.5, and 2 Hz, respectively. As shown in Fig. 4.20(c), λ increases with an increase in frequency, and the sample under the highest frequency of 2 Hz exhibits a higher λ. After a few cycles, λ is stable under all ranges of frequencies. A similar trend of damping was obtained with an increase in CSR and effective stress (Dai et al. 2022), where the soil was improved using cement. It can be seen in Fig. 4.20(d) that G/G_{max} decreases with increases in *N* for all the frequencies, but the variation of G/G_{max} is less with shear strain for *N* number of cycles when the frequency is low.

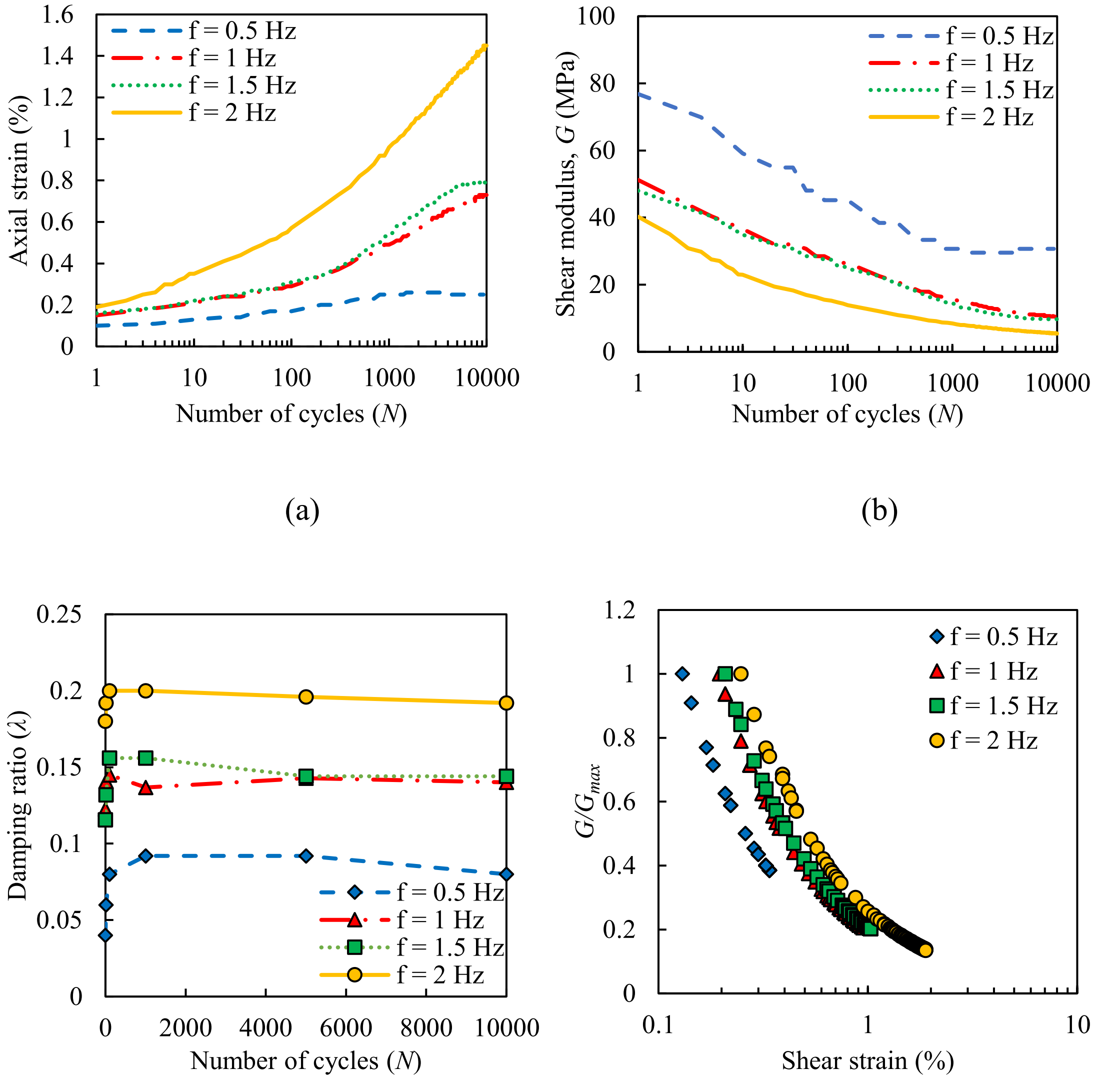

(a) (b)

(c) (d)

Fig. 4.20 Effect of frequency on the dynamic parameters (S:D = 16:4; curing time = 28 days; CSR = 1; CP = 100 kPa): (a) strain response with *N*; (b) variation of *G* with *N*; (c) variation of *λ* with *N*; (d) variation of G/G_{max} with shear strain.

4.3.4.5 Effect of change in confining pressure (CP)

To investigate the effect of CP on kaolin clay stabilized with optimum geopolymer content, three series of CP (i.e., 50, 100, and 200 kPa) were selected for cyclic triaxial testing. Fig. 4.21(a) presents the axial strain response of geopolymer-stabilized clay with *N* tested at different CP, keeping the other parameters constant. It can be seen that with the increase in CP, axial strain accumulation is also less with the increase in the number of cycles. Under the same number of stress cycles, there is a considerable increment in *G* with the increase in CP, as shown in Fig. 4.21(b). Furthermore, G_{max} increased by 55% when CP was increased from 50 to 200 kPa. With the increase in CP, more lateral confinement is provided, increasing the contact area and decreasing the deformation tendency between the clay particles, preventing the accumulation of axial strain. The lack of accumulation of axial strain increases the load-bearing capacity and dynamic shear modulus (Choobbasti et al. 2018; Du et al. 2021). On the other hand, less damping was observed with an increase in CP (Fig. 4.21(c)). With the increase in the number of cycles, the same trend of λ as of other parameters (S:D ratio, CSR, frequency) was observed while studying the effect of CP. The change in G/G_{max} with shear strain for *N* number of cycles was found to be minimum and within a narrow range when applied CP was increased from 50 kPa to 200 kPa as shown in Fig. 4.21(d). This was consistent with the study reported by (Acar and Asce 1987; Kumar et al. 2018; Wang et al. 2019).

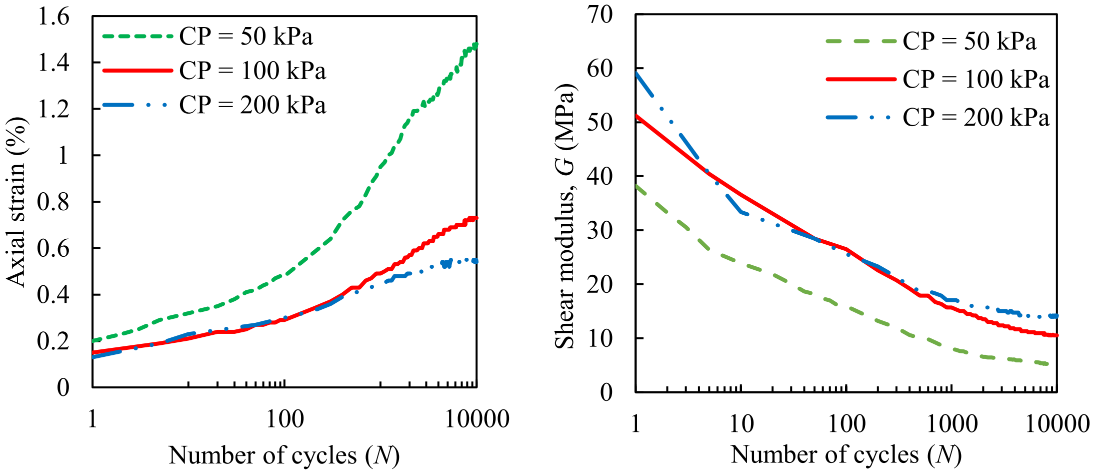

(a) (b)

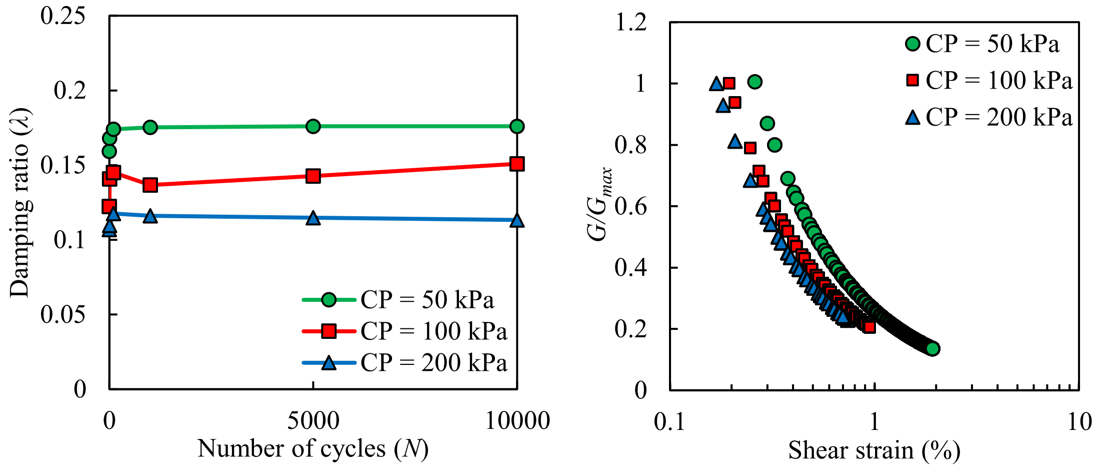

(c) (d)

Fig. 4.21 Effect of CP on the dynamic parameters (S:D = 16:4; curing time = 28 days; CSR = 1; frequency = 1 Hz): (a) strain response with *N*; (b) variation of *G* with *N*; (c) variation of *λ* with *N*; (d) variation of G/G_{max} with shear strain.

4.3.4.6 Empirical model and validation for dynamic shear modulus

The Martin-Davidenkov model proposed by (Martin and Seed, 1982) is used in this study for the validation of test results. The model was derived from the Hardin-Drnevich model (Hardin and Drnevich, 1972) as this model describes the relationship between dynamic shear modulus and shear strain and can be written as Eq. (4):

$$\frac{G}{G_{\max}} = 1 - \left[\frac{(\gamma/\gamma_r)^{2B}}{1+(\gamma/\gamma_r)^{2B}}\right]^{A} \tag{4}$$

Where A, B, γ_r are the dimensionless fitting curve parameters, G/G_{max} is the degradation index, and γ is the shear strain developed during dynamic loading. When putting A = 1, B = 0.5, and γ_r = reference strain, the model is degenerated into the Hardin-Drnevich model.

Fig. 4.22 presents the G/G_{max} variation with shear strain obtained from experimental results compared with non-linear fitting model curve results for all the CSR (0.5, 1, 1.5, and 2) and CP (50, 100, and 200 kPa) considered in the study. Table 4.3 shows the three dimensionless fitting parameters determined using non-linear fitting analysis, with correlation coefficient (R^2) ranging from 0.94 to 0.96. It can be seen that the trend of the model fitted well with the experimental results as the R^2 value under each regression is high, which means that the dynamic shear modulus of the geopolymer stabilized kaolin clay could be predicted well by the Martin-Davidenkov model. Also, the p-value obtained for all the tests was less than 0.0001, indicating that the applied model is statistically significant. The fitting parameters A, B, and γ_r values range from 0.55-1.26, 0.04-0.53, and 0.12-0.74, respectively.

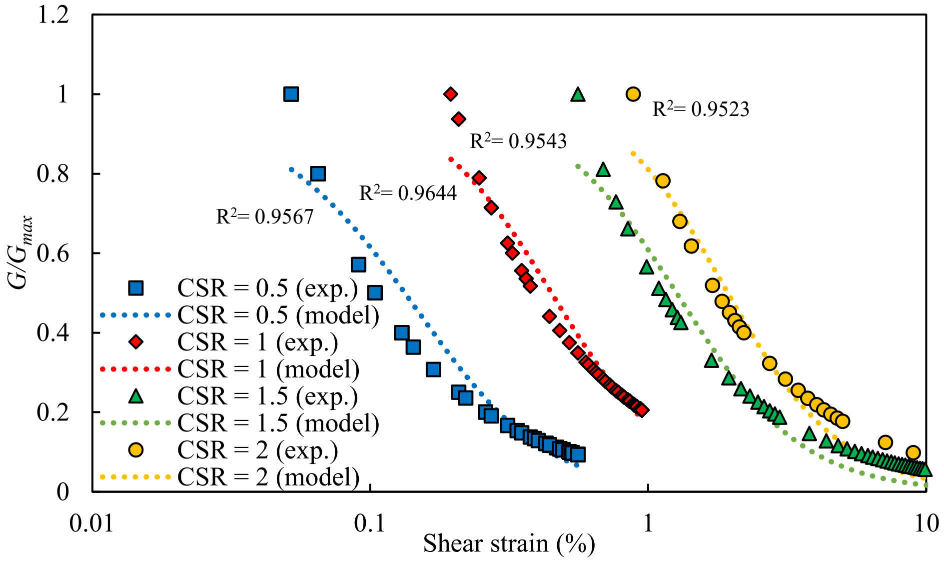

(a)

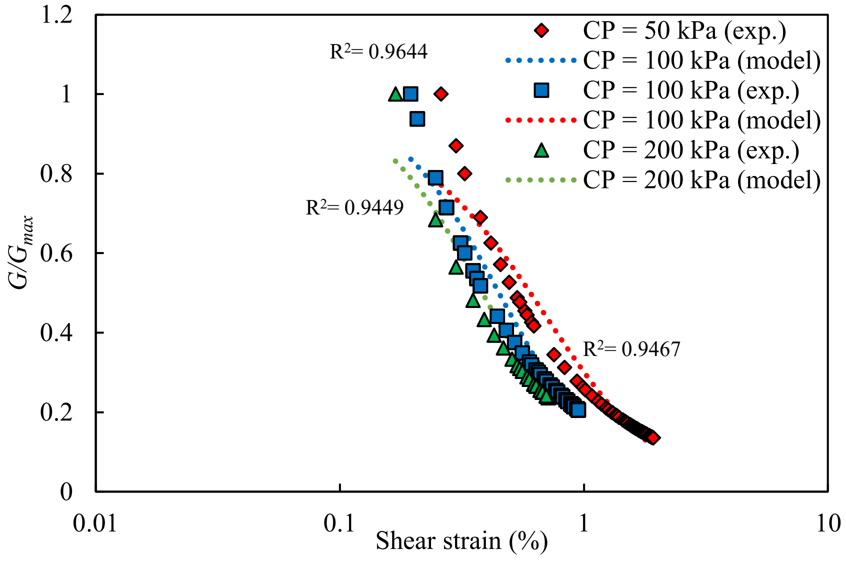

(b)

Fig. 4.22 Comparison between experimental data and fitting curve results of dynamic shear modulus for: (a) CSR; (b) CP.

Table 4.3 Values of non-linear fitting parameters *A*, *B*, and γ_r used in the Martin-Davidenkov model.

CSR	CP (kPa)	*A*	*B*	γ_r	Correlation coefficient (R^2)	*p-value*
0.5	100	0.62	0.53	0.13	0.9567	<0.0001
1	100	0.95	0.1	0.14	0.9644	<0.0001
1.5	100	0.84	0.17	0.59	0.9543	<0.0001
2	100	1.26	0.2	0.74	0.9523	<0.0001
1	50	0.55	0.04	0.2	0.9467	<0.0001
1	200	0.94	0.1	0.12	0.9449	<0.0001

(p-value ≤ 0.05 indicates statistically significant at the 95% confidence limit)

4.3.5 Microstructural analysis

4.3.5.1 Evaluation of chemical bond using FTIR

The FTIR spectrum of the geopolymer-treated kaolin clay with different alkali activator ratios of NH and NS and precursor (S:D) ratio 16:4 cured at 28 days are shown in Fig.

4.23. The characteristic peaks observed in the spectrum between 3795 and 3694 correspond to the bending vibrations of H-O group indicating the presence of $Ca(OH)_2$. The significant bands at 3430 cm^{-1} and 1630 cm^{-1} are attributed to the stretching vibrations of the H-OH group, indicating the water molecules common in the aluminum silicate network (Fernandez et al. 2005). This indicated the formation of a geopolymerization product into the specimen. The peaks obtained at 1448 cm^{-1} and 791 cm^{-1} wavenumber show the asymmetric stretching bonds of the O-C-O group, which are indicative of the presence of $CaCO_3$ (García Lodeiro et al. 2009). The peaks around the wavenumber of 1100 cm^{-1}, 1000 $cm^{-1,}$ and 912 cm^{-1} show the strong absorption band related to the asymmetric stretching vibration of the Si-O-T band (T: tetrahedral Si or Al) (Abdalqader et al. 2016; van Jaarsveld et al. 2002). These peaks are strong in the NH:NS ratio of 25:75 specimen and are related to nano-structural changes in the silicate network, providing evidence of higher geopolymer (C-A-S-H and C-S-H) gel formation. The peaks obtained at 693 cm^{-1} and 534 cm^{-1} indicate the stretching vibration of Si-O-Al in the AlO_4 group that could be related to the formation of C-A-S-H gel (Zhang et al. 2012). The peaks at 467 cm^{-1} and 430 cm^{-1} are attributed to the in-plane bending vibration of the Si-O-Si band of SiO_4 tetrahedra (Voll et al. 2001). The peaks observed in NH:NS ratio of 25:75 are more intense, showing that a geopolymer reaction takes place that is reflected in compressive strength enhancement.

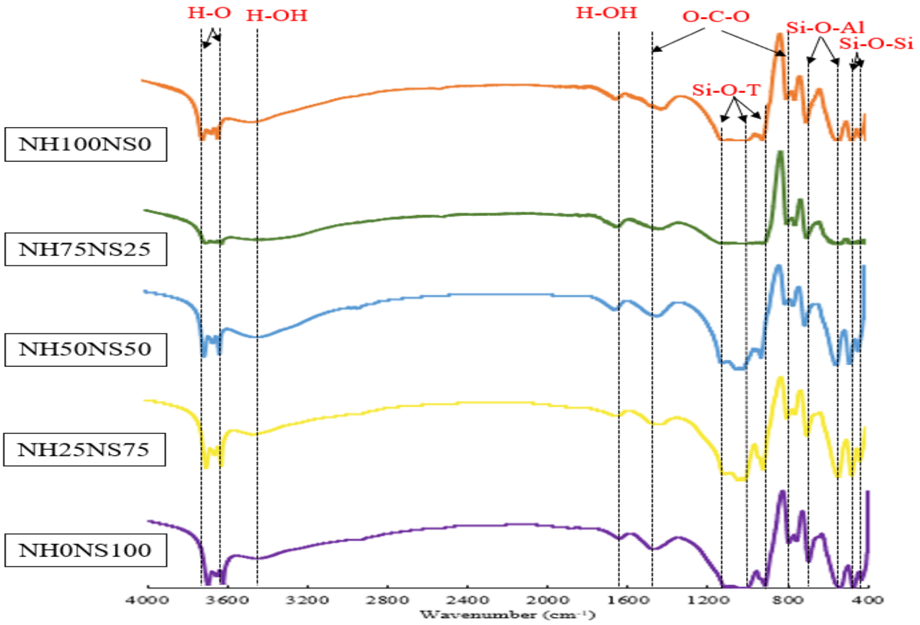

Fig. 4.23 FTIR spectrum of stabilized soil with different ratios of NH and NS with an S:D ratio of 16:4 after 28 days of curing.

4.3.5.2 Scanning Electron Microscopy test results

Microstructure analysis was conducted using a scanning electron microscope (SEM) to understand the geopolymer mechanism better. The SEM image analysis of the geopolymer-treated kaolin clay with different alkali activator ratios of NH and NS and precursor (S:D) ratio 16:4 cured at 28 days are shown in Fig. 4.24. To understand the effect of NH and NS on the geopolymerization process, microstructural analysis using SEM test was conducted on the 28 days cured representative specimens. It was observed that the pore size in the NH100NS0S16D4 specimen is larger, and with an increase in NS, the pore size is reduced. Also, the formation of C-A-S-H and N-A-S-H increases with an increase in NS. It can be seen that a well-compacted and dense structure of geopolymer gel is formed in the NH25NS75S16D4 specimen, and the pores are filled with C-A-S-H and N-A-S-H gel. Its dense gel structure formation with reduced pores confirms the attainment of the highest compressive strength in the specimen. The formation of flakes of geopolymer gel can be seen in the NH0NS100S16D4 specimen, indicating a considerable number of micropores, which shows that the particles are not bonded and negatively affect the compressive strength.

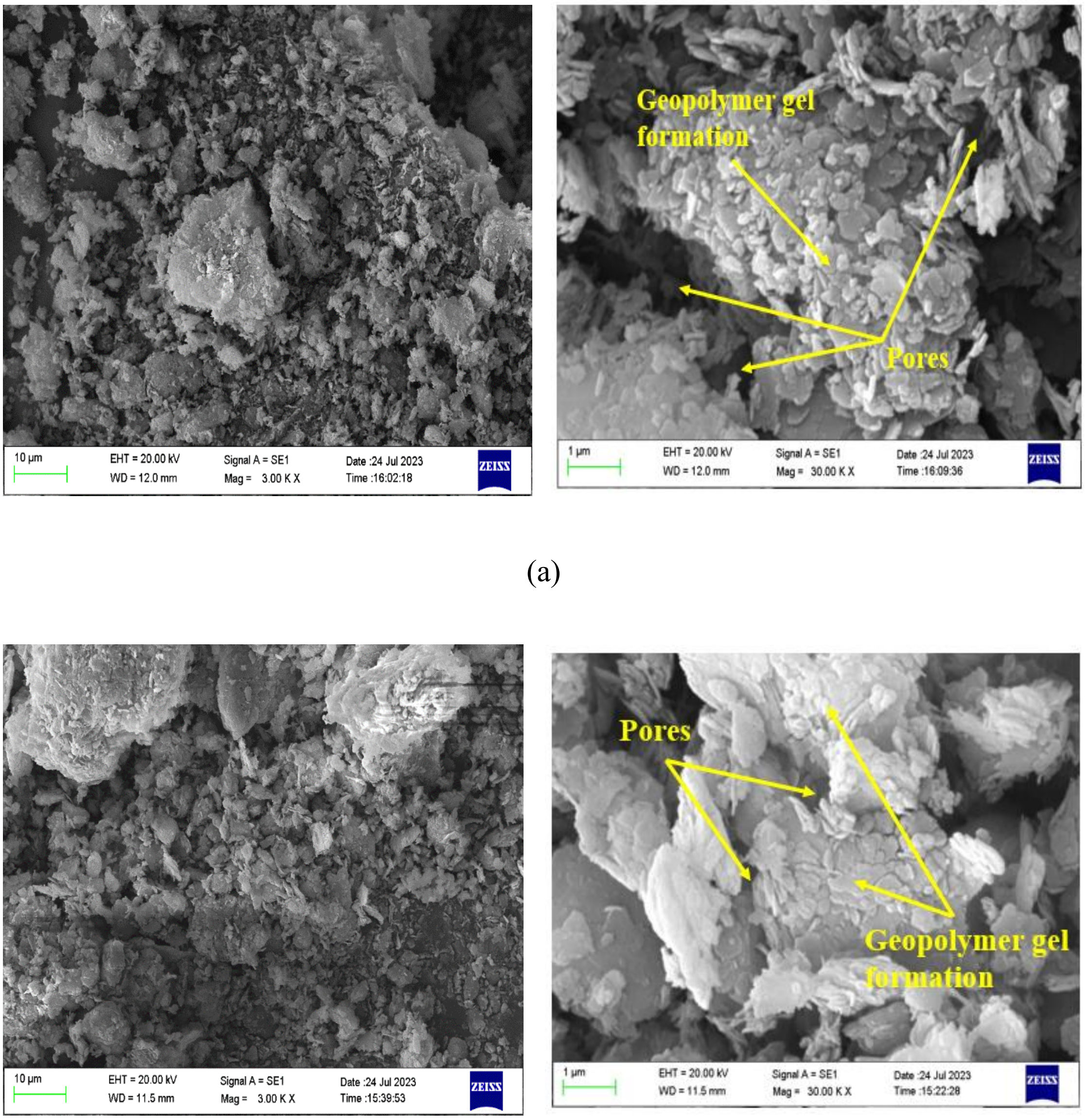

(a)

(b)

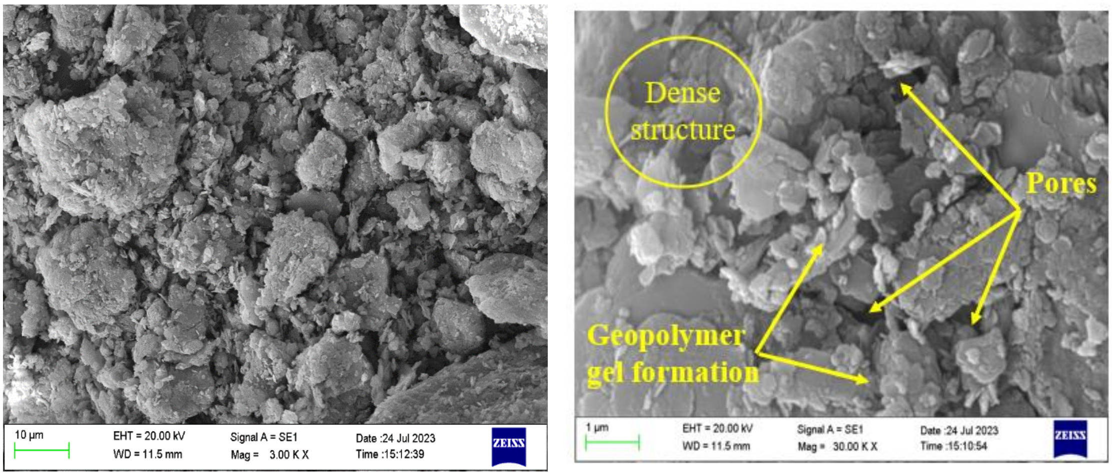
10 µm
EHT = 20.00 kV
WD = 11.5 mm
Signal A = SE1
Mag = 3.00 K X
Date :24 Jul 2023
Time :15:12:39
ZEISS
Dense structure
Pores
Geopolymer gel formation
1 µm
EHT = 20.00 kV
WD = 11.5 mm
Signal A = SE1
Mag = 30.00 K X
Date :24 Jul 2023
Time :15:10:54
ZEISS

(c)

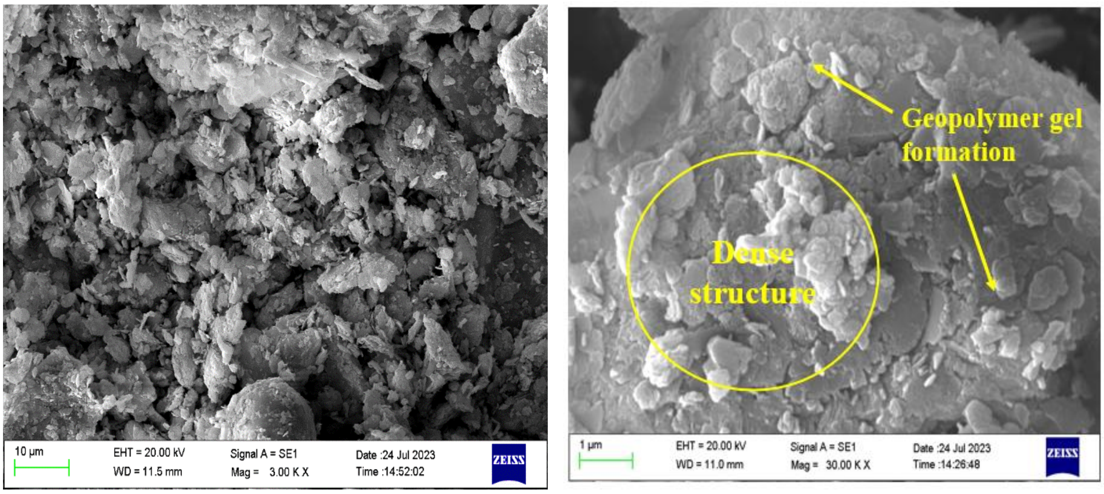
10 µm
EHT = 20.00 kV
WD = 11.5 mm
Signal A = SE1
Mag = 3.00 K X
Date :24 Jul 2023
Time :14:52:02
ZEISS
Geopolymer gel formation
Dense structure
1 µm
EHT = 20.00 kV
WD = 11.0 mm
Signal A = SE1
Mag = 30.00 K X
Date :24 Jul 2023
Time :14:26:48
ZEISS

(d)

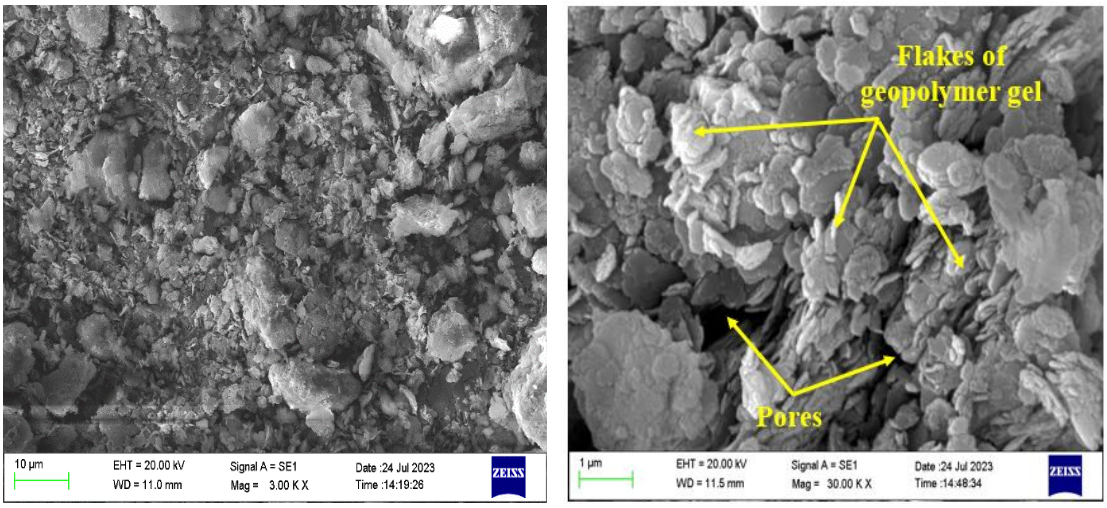
10 µm
EHT = 20.00 kV
WD = 11.0 mm
Signal A = SE1
Mag = 3.00 K X
Date :24 Jul 2023
Time :14:19:26
ZEISS
Flakes of geopolymer gel
Pores
1 µm
EHT = 20.00 kV
WD = 11.5 mm
Signal A = SE1
Mag = 30.00 K X
Date :24 Jul 2023
Time :14:48:34
ZEISS

(e)

Fig. 4.24 The SEM spectra of the selected samples of (a) NH100NS0S16D4, (b) NH75NS25S16D4, (c) NH50NS50S16D4, (d) NH25NS75S16D4 and (e) NH0NS100S16D4 after the curing of 28 days.

Fig. 4.25 shows the SEM images of the kaolin clay with a water content of 1LL stabilized using geopolymer with different ratios of S and D (precursor) cured for 28 days. The main cementation reaction process was found to occur during 28 days of curing time (Phetchuay et al., 2016b). As aluminosilicates get dissolved by the alkaline activation process, C-A-S-H and N-A-S-H gel and three-dimensional chain networks connecting the particles are formed. With a few partially reacted zones between the unreacted particles, geopolymer gels have been identified in all samples. It is evident that the addition of D in S efficiently activates and creates cementitious products exhibiting a closed structure with a strong contact link between the clay particles. Geopolymerization formed a denser morphology and homogeneous C-A-S-H gel structure that enhances the strength and contributes to improving the cyclic loading resistance of the treated clay. For the sample stabilized with an S:D ratio of 16:4, the geopolymers gel matrix appeared to be denser and more connected, which was also reflected by the UCS test results.

The result of SEM along with EDS of the geopolymer stabilized clay with an S:D ratio of 16:4 is presented in Fig. 4.26. According to the EDS test results, the major chemical elements were O (55.42%), Si (19.65%), Al (12.79%), Ca (4.34%), Na (4.6%), and Mg (3.2%), indicating the presence of significant quantities of amorphous N-A-S-H and C-A-S-H gels in the geopolymer stabilized clay. With the addition of D in S, the CaO content increases, producing amorphous C-A-S-H gels that reduce microstructural porosity and strengthen the geopolymer-stabilized clay.

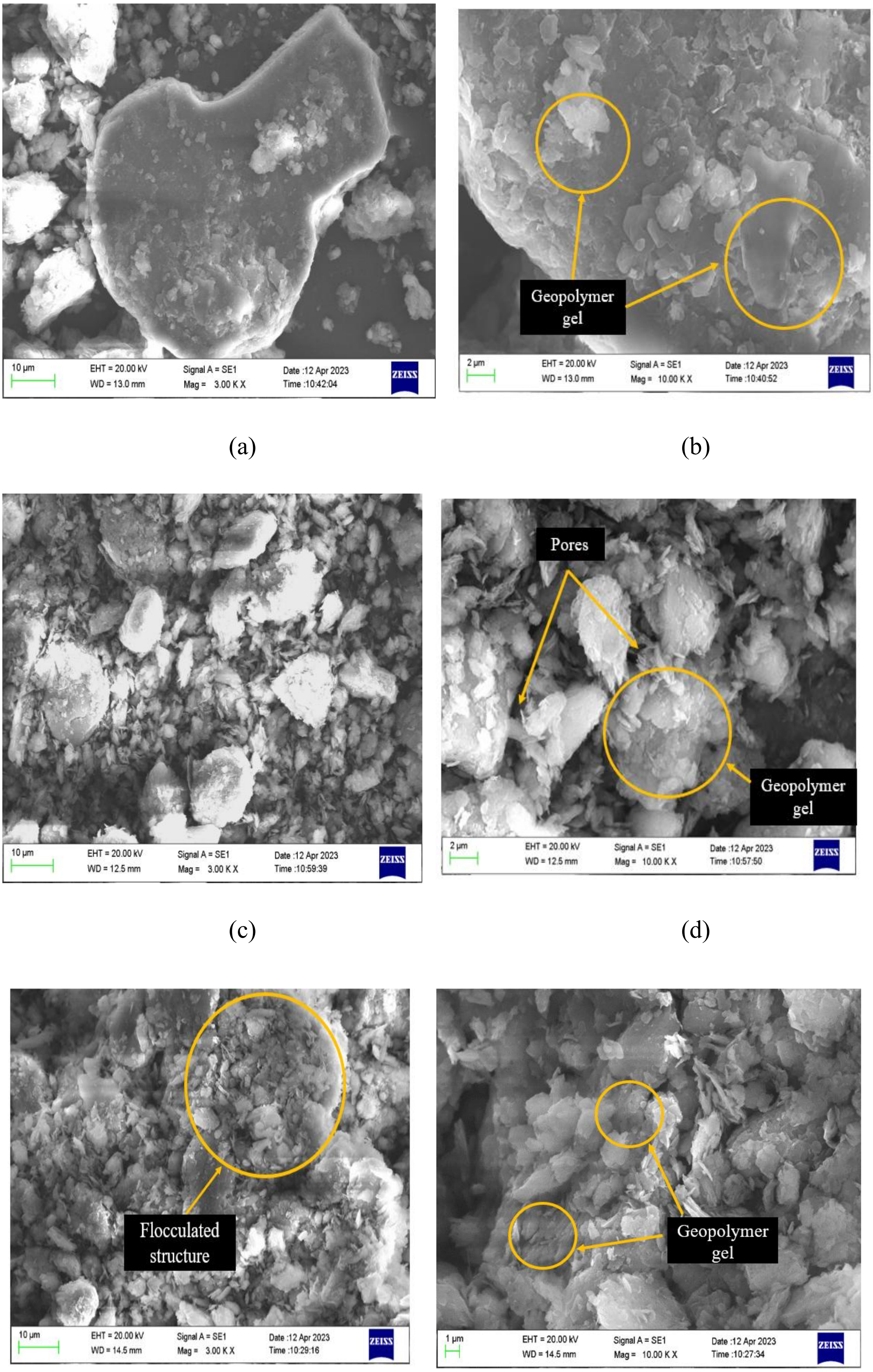
10 µm
EHT = 20.00 kV
WD = 13.0 mm
Signal A = SE1
Mag = 3.00 K X
Date :12 Apr 2023
Time :10:42:04
ZEISS
Geopolymer gel
2 µm
EHT = 20.00 kV
WD = 13.0 mm
Signal A = SE1
Mag = 10.00 K X
Date :12 Apr 2023
Time :10:40:52
ZEISS
10 µm
EHT = 20.00 kV
WD = 12.5 mm
Signal A = SE1
Mag = 3.00 K X
Date :12 Apr 2023
Time :10:59:39
ZEISS
Pores
Geopolymer gel
2 µm
EHT = 20.00 kV
WD = 12.5 mm
Signal A = SE1
Mag = 10.00 K X
Date :12 Apr 2023
Time :10:57:50
ZEISS
Flocculated structure
10 µm
EHT = 20.00 kV
WD = 14.5 mm
Signal A = SE1
Mag = 3.00 K X
Date :12 Apr 2023
Time :10:29:16
ZEISS
Geopolymer gel
1 µm
EHT = 20.00 kV
WD = 14.5 mm
Signal A = SE1
Mag = 10.00 K X
Date :12 Apr 2023
Time :10:27:34
ZEISS

(a) (b)

(c) (d)

(e) (f)

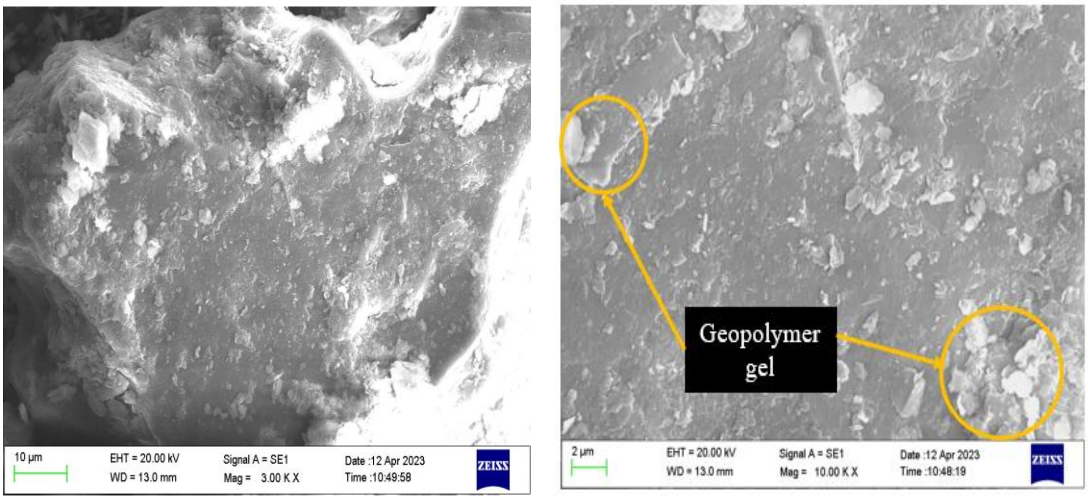

(g) (h)

Fig. 4.25 SEM microstructure image of geopolymer-treated kaolin clay with different ratios of S:D after 28 days of curing: (a), (b) S:D = 20:0; (c), (d) S:D = 18:2; (e), (f) S:D = 16:4; (g), (h) S:D = 14:6.

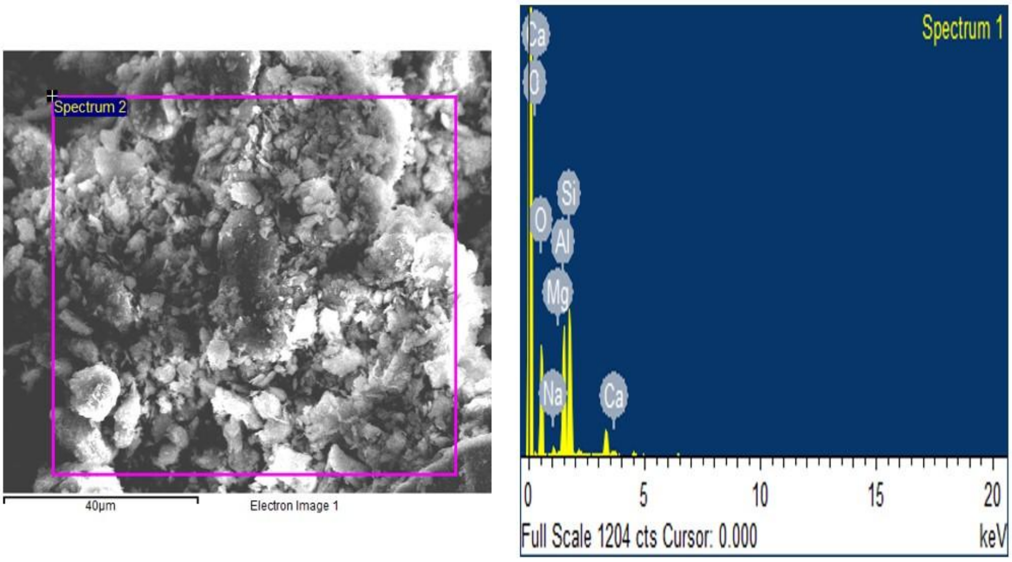

Fig. 4.26 SEM with EDS result of geopolymer-treated kaolin clay with an S:D ratio of 16:4 after 28 days of curing.

4.3.6 Toxicity Characteristic Leaching Procedure (TCLP) analysis

The TCLP test results of industrial waste material (GGBS and dolomite) and geopolymer-treated kaolin clay after 28 days of curing under room temperature are presented in Table 4.4. The concentration of heavy metals such as chromium (Cr), copper (Cu), nickel (Ni), zinc (Zn), arsenic (As), cadmium (Cd), mercury (Hg), and lead (Pb) were determined using TCLP test. The results were compared with the standard concentrations of heavy metals set by the US Environmental Protection Agency (USEPA 1992) given in Table 4.4. The heavy metal leachate of GGBS, dolomite, and geopolymer stabilized specimens was much less than the standard concentration of heavy metals for non-hazardous materials. Therefore, it can be concluded that GGBS and dolomite-based geopolymer can effectively stabilize the soft kaolin clay by improving the physical properties of soil without causing a harmful effect on the environment.

Table 4.4 Results of TCLP analysis.

Specimen ID	**Concentration in TCLP test (mg/l)**							
	Cr	Cu	Ni	Zn	As	Cd	Hg	Pb
Regulatory EPA limit	5	25	25	25	5	1	0.2	5
GGBS	0.04	0.02	0.02	<0.01	<0.01	<0.01	<0.01	<0.01
Dolomite	0.239	0.02	0.498	1.395	<0.01	<0.01	<0.01	<0.01
NH25NS75S20D0	0.732	<0.01	0.396	0.871	<0.01	<0.01	<0.01	<0.01
NH25NS75S18D2	0.120	<0.01	0.579	0.779	<0.01	<0.01	<0.01	<0.01
NH25NS75S16D4	0.278	<0.01	0.357	0.734	<0.01	<0.01	<0.01	<0.01
NH25NS75S14D6	0.276	<0.01	0.473	0.946	<0.01	<0.01	<0.01	<0.01

4.4 Summary

The present research investigates the utilization of dolomite with GGBS as a novel environmentally friendly geopolymer precursor to stabilize soft kaolin clay. The influential factors, such as the percentage of precursor, GGBS and dolomite ratios, NH and NS mass ratio, L/P ratio, water content of kaolin clay and curing period, were studied using UCS and pH tests. Furthermore, the static and cyclic triaxial stress-strain characteristics of the kaolin clay stabilized with optimum NH:NS mass ratio with different ratios of S:D based geopolymer was studied.

Dolomite substitution in GGBS has the potential to increase strength, as evidenced by the observed improvement in strength. Dolomite accelerates the geopolymerization process and offers more nucleation sites for the precipitate of C-S-H and C-A-S-H.

The optimum mix was determined to consist of an 8M NaOH concentration, a 25:75 NH:NS ratio, a 16:4 S:D ratio (precursor/kaolin clay = 20%), and a 1 L/P ratio. UCS values of 2.75 MPa, 1.47 MPa, and 1.21 MPa for water contents of 0.8LL, 1LL, and 2LL, respectively, indicates that the geopolymer process can significantly change the properties of soft soil. Furthermore, the findings of the TCLP test showed that the concentration of leached heavy metals in dolomite, GGBS and GGBS-dolomite based geopolymer was below the USEPA limit.